

INSIGHT: Interpretable Semantic Hierarchies in Vision-Language Encoders

Kai Wittenmayer, Sukrut Rao, Amin Parchami-Araghi, Bernt Schiele, Jonas Fischer
 Max Planck Institute for Informatics, Saarland Informatics Campus, Saarbrücken, Germany
 {kwittenm, sukrut.rao, mparcham, schiele, jonas.fischer}@mpi-inf.mpg.de

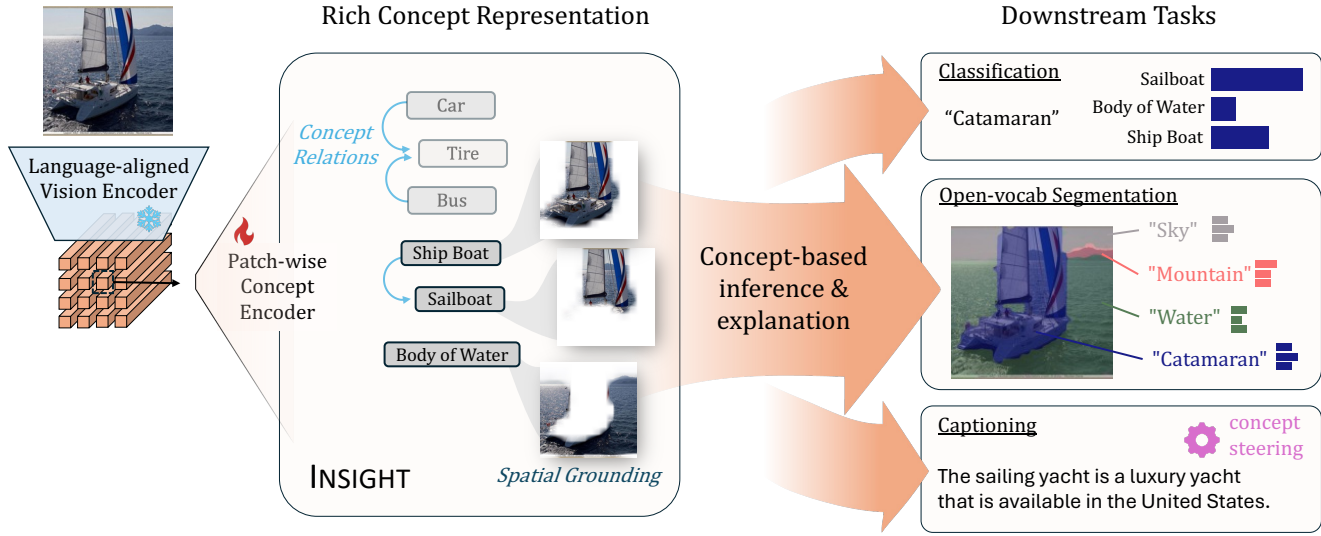


Figure 1. **INSIGHT provides rich conceptual explanations for vision foundation model tasks.** Our model provides a **hierarchical concept representation** (e.g. ‘Sailboat’ concept is a child of ‘Ship Boat’) with **local, spatially grounded** concepts that are automatically named. These concepts enable INSIGHT to provide concept-based explanations for decision-making across vision tasks.

Abstract

Language-aligned vision foundation models perform strongly across diverse downstream tasks. Yet, their learned representations remain opaque, making interpreting their decision-making hard. Recent works decompose these representations into human-interpretable concepts, but provide poor spatial grounding and are limited to image classification tasks. In this work, we propose INSIGHT, a language-aligned concept foundation model that provides fine-grained concepts, which are human-interpretable and spatially grounded in the input image. We leverage a hierarchical sparse autoencoder and a foundation model with strong semantic representations to automatically extract concepts at various granularities. Examining local co-occurrence dependencies of concepts allows us to define concept relationships. Through these relations we further improve concept naming and obtain richer explanations. On benchmark data, we show that INSIGHT provides performance on classification and segmentation that is

competitive with opaque foundation models while providing fine-grained, high quality concept-based explanations. Code is available at <https://github.com/kawi19/Insight>.

1. Introduction

Language-aligned vision foundation models such as CLIP [53, 62, 73] serve as powerful feature extractors that perform strongly across tasks such as zero shot classification and open-vocabulary semantic segmentation. Such models also serve as vision encoders for large vision-language models [13, 32, 35] and generative models. However, their representations are opaque, which hinders interpreting their decision-making. Interpretability is, however, key for human users, especially safety critical applications. There, explanations of decision-making can help to understand whether a model is right for the right reasons, increase trust in a model’s prediction, and investigate why a model got wrong or ended in harmful decisions.

Recent works [2, 33, 57, 72] aim to decompose repre-

sentations of foundation models into human-interpretable concepts and achieve transparency of these models at unprecedented scale. However, extracted concepts are not properly grounded in the input image [2, 57, 72] and often active as a result of spurious correlations, harming interpretability. Moreover, they only provide a limited range of granularity of concepts [2, 33, 57] and spatial coverage of those [2, 57, 72], and inter-concept dependencies are not examined even when using hierarchical priors [72]. Textual concept labels, when assigned [2, 57], often stem from a limited vocabulary that is not tailored for large-scale and fine-grained conceptual diversity. Apart from these limitations of the given explanations, existing works were only considering interpretable image classification, whereas the underlying foundation model is capable of much more.

In this work, we address these issues and propose INSIGHT, a language-aligned concept foundation model that provides named concepts at multiple granularities. These concepts are spatially grounded in the image and organized into hierarchies with explicit inter-concept dependencies. To do this, we develop a Matryoshka sparse autoencoder [6, 72] to represent local, DINOised CLIP features [64], which gives spatially localized and human-aligned concepts from coarse to fine granularities. Examining co-occurrences of local concept activations we discover parent-child relationships between concepts that provide further insights into the learned semantics. We further use these relations to refine concept labeling towards more accurate and meaningful textual concept labels. Our model enables interpretable decision-making for a variety of down-stream tasks typical for a language-aligned vision foundation model (see Fig. 1).

Contributions. (1) We propose to learn hierarchical concept extraction to obtain **human-interpretable concepts at diverse granularities** that are **spatially well-grounded** in the input. (2) We show how to extract **explicit hierarchical relations** between those concepts that improve the understanding of the model. (3) We propose an **improved concept labeling scheme** that explicitly takes parent-child relationships from this hierarchy into account. (4) Putting these together, we propose INSIGHT, a language-aligned foundation-like model that enables **interpretable decision-making across downstream tasks** such as classification, open-vocabulary segmentation, and image captioning.

On benchmark data and through a human user study we show that in contrast to state-of-the-art, INSIGHT yields concepts that are more quantitatively and qualitatively consistent, spatially more localized, and meaningfully named (Tab. 1, Fig. 5). We further show that this added interpretability does not come with a degradation of performance across various downstream tasks. On image classification tasks INSIGHT yields performances competitive with the state-of-the-art concept-based and opaque baseline

models (Tab. 2). On a light-weight image captioning task, INSIGHT performs similar to its opaque backbone and enables steering (Fig. 6). INSIGHT also enables interpretable open-vocabulary segmentation that is on par with opaque foundation model alternatives (Tab. 3).

2. Related work

Vision-language models (VLMs) such as CLIP [14, 26, 53], ALIGN [27], CoCa [70], and SigLIP [62, 73] learn vision and text encoders that share a semantic latent space. Such models are typically trained on billions of paired image-text data through contrastive learning, yielding powerful but opaque language-aligned visual representations enabling tasks such as open-vocabulary classification and semantic segmentation. Our proposed method INSIGHT is such a language-aligned vision encoder, but trained to provide a human-interpretable concept representation space.

Concept extraction methods aim to decompose learned representations from encoders into human-interpretable concepts through, e.g., clustering [23, 31, 45], non-negative matrix factorization [21] or a learned concept dictionary that is image-specific [2] or shared across images [33, 49, 57, 72]. The latter, in particular, have been applied to VLMs, but (1) lack spatial grounding of concepts to the image [2, 57, 72], (2) learn a flat hierarchy of concepts [2, 33, 57], or (3) use a limited vocabulary and imprecise names [57]. Our INSIGHT, in contrast, learns a rich set of spatially grounded concepts with explicit parent-child relationships that are named using a large fine-grained vocabulary taking such relationships into account, yielding a significantly more accurate, localized, and interpretable concept decomposition.

Sparse autoencoders (SAEs) [3, 16] are models that aim to learn a dictionary of human-interpretable concepts from a latent space. These consist of an affine encoder and decoder that map features to a sparse high-dimensional space of concepts typically trained through a reconstruction and sparsity loss. SAEs have been shown a useful tool to understand large language models (LLMs) [3, 16] as well as vision models [57, 72]. Recent works suggested alternative sparsity objectives [5, 22, 54, 55] and architectural priors for concept hierarchies [6, 72] to improve SAE representations. Here, we combine the best of both worlds and use Matryoshka SAEs [6] with a BatchTopK objective [5] to extract high quality, localized, and hierarchical concepts.

Concept-based classification models such as concept bottleneck models (CBMs) [1, 30, 44, 57, 71] and visual prototype-based methods [11, 18, 42, 67] learn concepts from a latent feature space to yield interpretable classification predictions. Where CBMs extract labeled, global concepts that are have shown to be often not correctly grounded in the image [25], prototypes are local visual features that

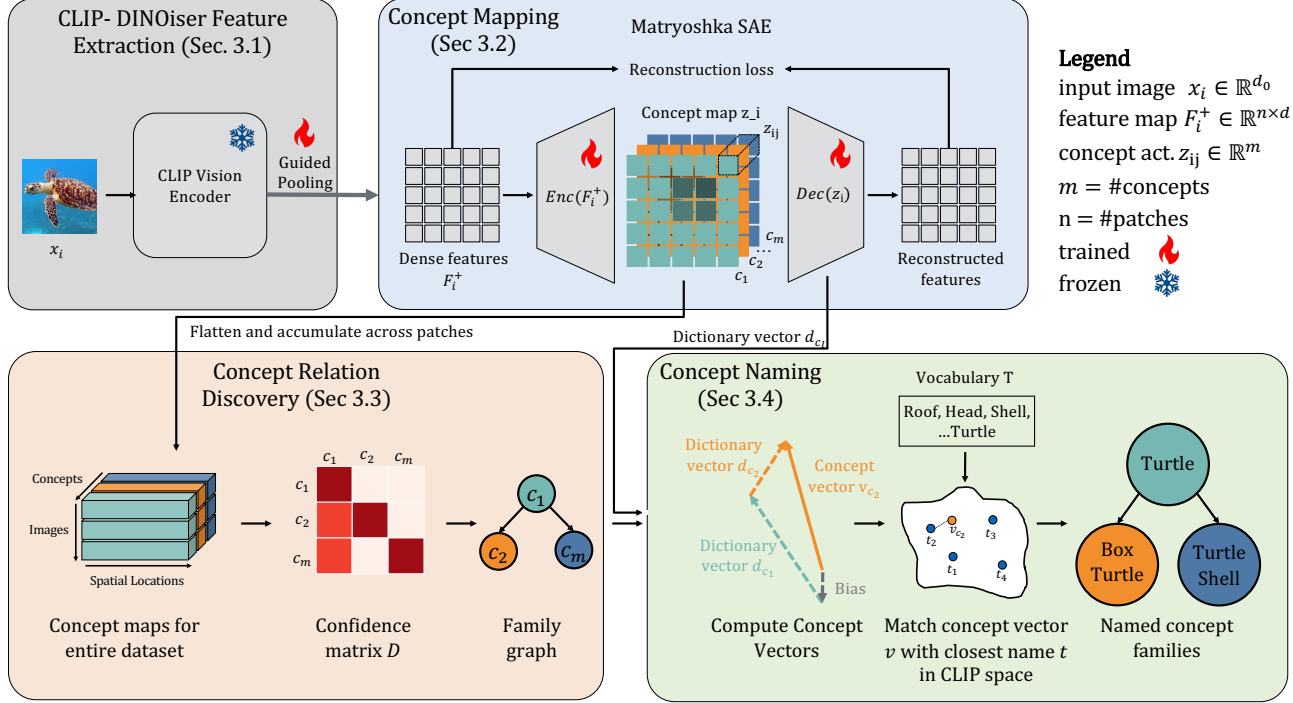


Figure 2. **Overview of INSIGHT.** We visualize our approach to represent human-interpretable, well localized, and consistent concepts of different granularities in a language-aligned vision foundation model. As backbone, we use pretrained CLIP-DINOiser [64] and extract concepts patch-wise by training a Matryoshka Sparse Autoencoder (SAE) without any supervision. From these learned concept representations, we discover concept relations through examining the co-occurrences of concepts within patches that allow more fine-grained interpretation of decision-making on downstream tasks. We further name the concepts with a Matryoshka-aware matching between concept representations and a large vocabulary of labels, taking the discovered concept relations into account.

have to be investigated by a user to understand their conceptual meaning. Our approach bridges the gap between the two and help construct inherently interpretable concepts that are labeled, can be global as well as local, and are well grounded in the input. Moreover, in the spirit of foundation models, INSIGHT enables downstream tasks beyond just classification.

3. INSIGHT: A language-aligned concept foundation model

To equip language-aligned vision foundation models with transparent, human-interpretable reasoning, we propose a semantically meaningful representation layer that encodes interpretable concepts. In a nutshell, we learn a *local* mapping from dense representation to human-interpretable concept space. This concept space is encouraged to represent *concepts at different levels of granularities*, so that we are able to discover locally consistent *concept hierarchies* describing part- or specification-relationships between concepts based on patch-wise concept co-occurrences (Fig. 2).

Specifically, we build on CLIP-DINOiser [64], a CLIP architecture that encodes images such that semantically similar regions, informed through DINO [8], share similar

representations (Sec. 3.1). To map this latent CLIP encoding to meaningful concepts at different levels of granularity, we modify the recently proposed Matryoshka Sparse Autoencoder (SAE), learning patch-wise interpretable concept representations in an unsupervised manner at scale (Sec. 3.2). From these interpretable concept representations, we show how to extract relations between concepts that reflect both specifications as well as part-relations through an analysis of local co-occurrence patterns (Sec. 3.3). Finally, we extend the existing concept vocabularies used for labeling, show how to improve concept labeling by leveraging our discovered concept relationships, and show that an architecture-aware text encoding is necessary for accurate labels (Sec. 3.4).

3.1. The CLIP-Dinoiser backbone

Despite being trained to produce image-level embeddings, it has been shown that [76] fine-grained local representations can also be extracted from the CLIP [53] vision encoder. Specifically, the patch token value vectors from the CLS attention of a CLIP ViT [19] can be repurposed as dense local embeddings. While having a global context, these still preserve a degree of spatial locality, but are noisy.

To address this, we adopt the guided pooling approach introduced for the CLIP-DINOiser architecture [63], which smoothens the representations of semantically similar patches. To do so, we can use the affinity patterns of self-supervised features, such as DINO [8], computed as inter-patch cosine-similarities $A^\xi \in [-1, 1]^{N \times N}$. This gives dense “DINOised” features F^+ for each patch p as

$$F_p^+ = \frac{1}{\sum_{q=1}^N A_{p,q}^\xi} \sum_{q=1}^N A_{p,q}^\xi \cdot F_q, \quad (1)$$

where N is the number of patches and F_q is the value vector of patch token q of the last attention. Intuitively, this pooling acts as a “voting system” that enforces consistency among semantically similar patches while “attenuating noisy features” [63].

To be effective at inference, Wysoczańska et al. [63] observed that CLIP features already have semantically meaningful information similar to DINO and suggest to train a small 3×3 convolutional layer $g : \mathbb{R}^d \rightarrow \mathbb{R}^{d'}, d' < d$ on transformer patch tokens of an intermediate layer ϕ^l to approximate the DINO affinity map A^ξ . In our case, we approximate A^ξ from the *final* CLIP layer L by

$$A^\phi = \frac{g(\phi^L(X))}{\|g(\phi^L(X))\|} \otimes \left(\frac{g(\phi^L(X))}{\|g(\phi^L(X))\|} \right)^T \quad (2)$$

for patch tokens X . The convolution g is learned through a binary-cross entropy loss between A^ϕ and binarized DINO affinities $A^\xi > \gamma$; we refer to App. B for more details.

At inference time, this only requires a single forward pass through CLIP ϕ , computing the affinity map A^ξ of the patch tokens using the trained convolution g , and applying it as weights (Eq. (2)) for guided pooling on the final patch tokens. This approach offers three advantages for concept extraction compared to CLIP. First, the extracted local embeddings are well aligned with CLIP’s language space, meaning that each spatial feature can still be directly associated with natural language descriptions through CLIP’s pretrained text encoder. Second, because these local embeddings are pooled from semantically coherent regions of the image, such regions frequently correspond to meaningful object parts or localized visual attributes. Third, this DINOising approach is, in principle, compatible with most language-aligned vision encoders, requiring only a lightweight convolutional adapter. Next, we will discuss how to map such DINOised feature maps to an interpretable concept space.

3.2. Unsupervised concept mapping through Matryoshka SAEs

To learn a mapping from the powerful latent representations of foundation models to human-interpretable concepts, we leverage sparse autoencoders (SAEs) [3]. These consist of a

light-weight linear layer as encoder, $\pi : \mathbb{R}^d \rightarrow \mathbb{R}^{d'}$ that describes an affine mapping from a d -dimensional input space, e.g., a CLIP space, to a sparse representation where each dimension ideally encodes a single interpretable concept. An affine mapping $\pi^{-1} : \mathbb{R}^{d'} \rightarrow \mathbb{R}^d$ then maps back to the input space, allowing to train this autoencoder architecture efficiently through a reconstruction loss such that

$$\pi^{-1}\pi(x) \approx x, \quad x \in \mathbb{R}^d. \quad (3)$$

A key detail of SAEs is an additional loss term that encourages sparsity of concept activation for each input x . We here use a version of the top- k approach, where at each forward pass all but the top- k most activating neurons on input x are set to zero. While not perfect, SAEs provide a very efficient and unsupervised method to learn a concept mapping, both of which are crucial at the scale of a foundation model.

In contrast to existing concept extraction approaches, we encode *each patch* through the autoencoder, which through the use of a semantically rich feature map as input allows to learn meaningful and well-grounded local concepts at scale. We use a BatchTopK [5] Matryoshka SAE [37, 72], which allows to flexibly distribute the capacity k of concepts across samples (here patch encodings) in a batch. It further adds an auxiliary reconstruction loss for different subsets of first l neurons in the concept layer, akin to a Matryoshka. Each subset of neurons by itself then needs to reconstruct the input. More formally, let $C = [1 \dots m]$ be the index set for the m neurons in the SAE concept layer and $l_j \in C$ indices until which we define a matryoshka shell. Then

$$\mathcal{L}_{rec}(F_p) = \sum_j \left\| \pi^{-1}(\pi(F_p)[1 : l_j]) - F_p \right\|_2^2, \quad (4)$$

where F_p are the latent features for patch p given by the backbone model and $\pi(F_p)[1 : l_j]$ sets all activations of neurons after index l_j to zero. In other words, each Matryoshka shell consisting of the first l_j neurons is trained to reconstruct the *full* latent features, which encourages that the smallest subset of neurons learns coarse, high-level information and higher-index neurons learn the *residual* fine-grained information on top of this coarse representation.

3.3. Co-occurrence based concept relationships

To discover concept relations, related work relies on predefined concept hierarchies or leveraged LLMs [48, 61] to order concepts in a hierarchical manner. However, predefined hierarchies or external ontologies may not reflect the structure that emerges in the data or the model’s reasoning process. By discovering concept relations directly from data, we avoid mismatches between imposed taxonomies and the representations that the model actually uses. This allows for a more faithful interpretation and avoids biases introduced by LLM- or human-curated ontologies.

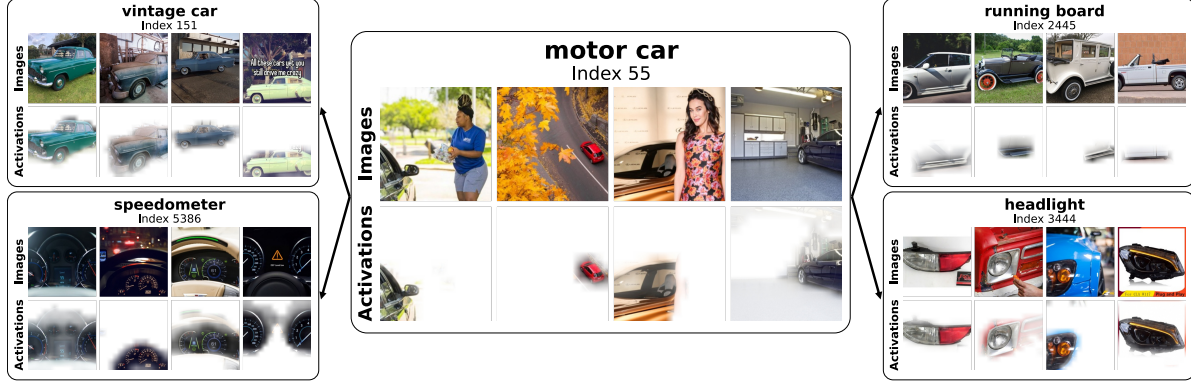


Figure 3. **A concept relationship subgraph.** The parent concept, ‘motor car’, is given as box in the center with children concepts arranged around it. For each concept, we provide the assigned label (top) and the top-4 most activating images (first row) along with their spatial localization (second row) based on concept activation strength per patch.

To represent hierarchies we define a *family* consisting of parent and child concepts, where parents represent more general concepts (e.g., “turtle”) and children capture more fine-grained or part-based specializations (e.g., “leatherback turtle”, “turtle shell”). A family is represented as a directed acyclic graph $\mathcal{G} = (V, E)$, where V is the set of *concepts*, $E \subseteq V \times V$ is the set of directed edges such that $(u, v) \in E$ denotes that u is a *parent* of v .

We take inspiration from Ye et al. [69], which used the co-occurrence of extracted document-level features in dense text embeddings of LLMs to reveal “feature families” as trees. Instead, we use concept activation patterns across patch embeddings to discover our relations. To adapt to visual hierarchies, our families are not constrained to trees, but nodes can have multiple parents, which is better suited to represent the relations described above. We extend their approach and consider confidence instead of simple co-occurrence, which allows to better define the orientation of a parent-child relation. More formally, let $\mathbb{1}_{ji} = \{\text{concept } c_j \text{ is activated in patch } i\}$ be an indicator variable, and A_{ji} the activation of concept c_j on patch i , then the weighted confidence matrix is

$$D_{j,j'} = \frac{\sum_i \mathbb{1}_{j'i} A_{ji}}{\sum_i A_{ji}}. \quad (5)$$

Note that we sum over all patches of *all images* in the data to get a general concept relationship graph.

An entry in D represents the weighted conditional probability of concept j' appearing given that concept j appeared in a patch. D is used as the weighted adjacency matrix for our graph. To remove weak associations, we prune edges with weights < 0.75 . The family graph is then obtained by inverting the direction of the (remaining) edges. This inversion ensures that edges consistently point from general, highly frequent concepts to specific, infrequent concepts. For this to work, our design with *local, well-grounded* con-

cepts is crucial as otherwise spatially unrelated concepts (e.g., *field* and *cow*) may incorrectly be assigned a family relationship merely due to spurious correlations in their image-level activations.

The discovered relations refine explanations through inter-concept dependencies and serve as a prior that allows to learn better concept labels discussed next.

3.4. Hierarchy-aware concept labeling

For human-understandable textual explanations of decision-making, previous approaches [57] suggested to learn labels for each concept neuron in an unsupervised fashion. Yet, their assigned labels often appear spurious and for open-set concept naming the vocabulary often too limited to reflect the fine-grained visual features that vision models can capture. Here, following the idea of Rao et al. [57], we leverage the language-aligned CLIP backbone to assign labels l_i based on maximum cosine similarity between CLIP text encoder representations \mathcal{T} of a text v from a pre-defined vocabulary V , and the concept dictionary vector for the target concept i , which is given by the SAE decoder weights π_i^{-1} . More formally, we obtain

$$l_i = \operatorname{argmin}_{v \in \mathcal{V}} \cos(\pi_i^{-1} + b, \mathcal{T}(v)), \quad (6)$$

where \cos is cosine similarity and b the SAE decoder bias.

This existing approach performs well for general concepts in the first Matryoshka group of the SAE, however, due to residual reconstruction of more fine-grained features in the Matryoshkas, requires an adapted dictionary vector reconstruction (see App. B). In essence, we need to take into account the residual dependencies between concepts, adding the dictionary weights of the fine-grained concepts to those of their super-concepts. Such super-concepts are given through the graph \mathcal{G} as any parent a of a target con-

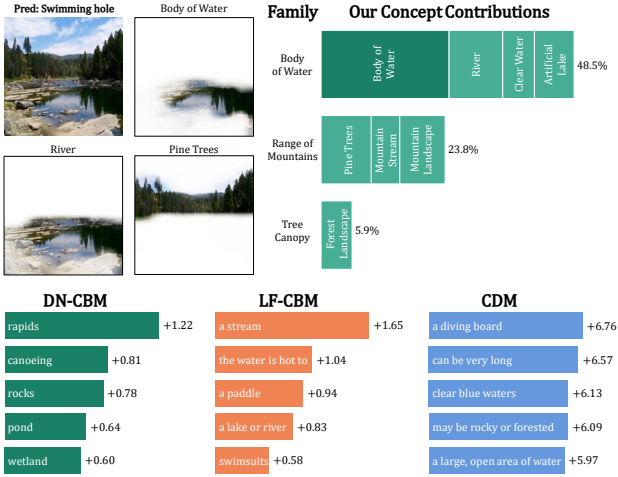


Figure 4. **Spatial grounding of concept-based explanations.** For an image of the "Swimming hole" Class of Places365 we show explanations of INSIGHT against existing method. For INSIGHT, we provide the parent concept (dark green) and its contributing children (light green) with percentage of contribution and the spatial grounding of the top-3 most contributing concepts. In contrast to our work, existing methods (bottom) show spurious concepts.

cept node i . More formally, we get

$$l_i = \operatorname{argmin}_{v \in \mathcal{V}} \cos \left(\sum_{a \in G, a \rightarrow i} \pi_a^{-1} \pi_i^{-1} + b, \mathcal{T}(v) \right), \quad (7)$$

where $a \rightarrow i$ means a is parent of i in \mathcal{G} . As vocabulary, we here consider the union of several datasets that lend themselves as concepts, which have been previously used in this context. Specifically, we use vocabularies from Brysbaert et al. [4], Muraki et al. [41], Oikarinen and Weng [43] and discuss filtering in App. B.

Putting all pieces together (Fig. 2), we obtain INSIGHT, a foundation-like vision model which extracts language-aligned, spatially grounded, and coarse-to-fine human-interpretable concepts from images for explainable downstream decision-making.

4. Experimental evaluation

We evaluate INSIGHT with ViT-B-16 CLIP-DINOiser backbone and compare the discovered concepts to state-of-the-art concept extraction methods using interpretability metrics on annotated datasets and conduct a human-user study to assess concept interpretability in Sec. 4.1 and provide details on metrics, data, and study design in App. A.

For downstream task evaluation, we consider image classification on Imagenet [17] and Places365 [74], where we compare to LF-CBM [44], LaBo [68], CDM [47], DCLIP [38], DN-CBM [57], D-CBM [51], CF-CBM [48], SALF-CBM [1] which are state-of-the-art concept-based inter-

Table 1. **INSIGHT discovers well-grounded concepts.** We compare against state-of-the-art concept extraction methods on data with available part annotation, including PartImageNet (Part) and Coco_stuff (Stuff) and measure localization of concepts to annotated parts (Locality), consistency of localization to same part across images (Consistency), and concept purity across parts (Impurity). Methods with * do not itself provide spatial localization, we use LRP to obtain spatial attributions. Best method in **bold**.

Methods	Locality \uparrow		Consistency \uparrow		Impurity \downarrow	
	Part	Stuff	Part	Stuff	Part	Stuff
SALF-CBM [1]	16.4	19.5	9.9	6.7	0.841	1.143
DN-CBM * [57]	18.7	17.9	9.3	5.7	0.761	1.235
MSAE * [72]	20.9	20.0	10.6	7.9	0.833	1.198
PatchSAE [33]	32.2	34.6	13.1	12.7	0.353	0.663
INSIGHT	44.3	44.5	15.3	13.1	0.333	0.539

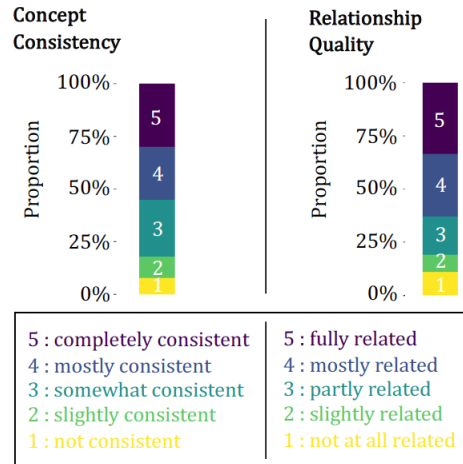


Figure 5. **Human User Study.** Results on Task 1 – Consistency evaluation (left) and Task 2 – Relationship evaluation (right) for 1000 neurons each covered with 5 users in Amazon MTurk. We provide the scale description given to the user at the bottom.

pretable models specifically designed for classification in Sec. 4.2. We further show that INSIGHT can be applied to yield meaningful image captions along with explanations for this caption grounded in the input in Sec. 4.3. Lastly, we consider open vocabulary segmentation (OVS) in Sec. 4.4, for which we compare to black-box VLM architectures [9, 28, 36, 56, 58, 60, 65, 66] specifically tailored OVS. None of the existing CBMs are capable of OVS.

We provide details on INSIGHT training in App. B and additional qualitative results in App. C.

4.1. Concept interpretability

INSIGHT discovers a large and interpretable space of 8192 concepts covering coarse to fine features and their relations. We provide an example relationship graphs of discovered concepts in Fig. 3, which shows visually well-grounded and meaningfully related concepts of varying granularity

and provide more examples in App. B.

Quantitatively, we confirm these initial observations in an evaluation on part-annotated datasets PartImagenet [24] and COCO-stuff [7] comparing to the recent state-of-the-art concept extraction methods SALF-CBM [1], DN-CBM [57], MSAE [72], and PatchSAE [33]. We measure how well concepts align with human-annotation as the maximum IoU between concept localization and annotated segments across all parts. Further, we measure how consistent a concept is localized to the same part across images by summing IoUs for one annotated part across images and taking the maximum over the parts. Lastly, we consider how semantically pure a concept is by computing the per-concept entropy of normalized activation values across annotated parts. We report the results in Tab. 1 and provide more details on metrics in App. A. INSIGHT consistently outperforms all considered competitors across datasets and metrics, confirming our qualitative observation. Especially in terms of locality, INSIGHT provides a huge improvement over existing works. Taking the results together, we confirm that **INSIGHT provides more interpretable, well-grounded concepts than previously possible**.

While relying on human-annotated part data for quantitative evaluation is an established benchmark in the field and provides a proxy for interpretability, ultimately we are interested in how well humans perceive and understand our discovered concepts. We conducted a large-scale human-user study covering 1000 concepts through Amazon MTurk. We partitioned concepts into five bins based on activation frequency, resembling the Matryoshka shells, and sampled concepts uniformly at random from each bin. In **Task 1**, we showed the top-5 most activating images of a concept along with its spatial grounding in each image and asked users to rate on a 5-point scale, where 5 is best. In **Task 2**, we asked users to evaluate the quality of a relationship discovered between two concepts, showing the top-3 most activating images and spatial grounding for both concepts, respectively. We then asked to rate how related the two concepts are on a 5-point scale, where 5 is best.

We show aggregated results in Fig. 5 and provide detailed study design and results in App. A. Overall, in both tasks users rated concepts mostly or completely consistent resp. related for more than half of the shown concepts. More than 80% of the evaluations assign *at least* somewhat consistent resp. related as a score (3 or higher). For an additional task of concept naming evaluation, we find that *free-form* text annotations given by users for a concept are significantly more similar to INSIGHT’s concept naming compared to a random baseline (App. A). Overall, this shows that our concept representation space, learned without any concept labels, **provides human users with consistent concepts and meaningful concept relations**.

4.2. Image classification

Table 2. **INSIGHT shows competitive classification performance while providing spatially grounded concepts.** We compare INSIGHT SOTA concept extraction methods and baselines on ImageNet (IMN) and Places365 (Places). “Spatial Grounding” indicates whether methods extract spatially grounded concepts (✓), partially local concepts (●), or global concepts only (✗). We show linear probe performance of INSIGHT on max- and mean-pooled concept activations across patches. Baseline results taken from Prasse et al. [51], we retrained INSIGHT on the same OpenAI-CLIP backbone, best method in **bold**.

Model	Spatial Grounding	IMN	Places
Linear Probe	-	80.2	55.1
Zero Shot	-	59.6	38.7
LF-CBM [44]	✗	75.4	48.2
LaBo [68]	✗	78.9	-
CDM [47]	✗	79.3	52.6
DCLIP [38]	✗	68.0	40.3
DN-CBM [57]	✗	79.5	55.1
D-CBM [51]	✗	70.5	50.9
CF-CBM [48]	●	78.5	-
SALF-CBM [1]	✓	76.3	49.4
INSIGHT	✓	78.9	55.4

Existing concept extraction methods are usually only designed and trained for image classification. To compare on common ground with such interpretable methods, we here consider image classification on ImageNet [59] and Places365 [74] by training a linear classification head on top of each model. We compare INSIGHT with LF-CBM [44], LaBo [68], CDM [47], DCLIP [38], DN-CBM [57], D-CBM [51], CF-CBM [48], SALF-CBM [1], most of which also rely on a CLIP backbone with ViT-B architecture. Apart from SALF-CBM and INSIGHT, none of the other approaches extracts spatially grounded concepts, but rather provide image-level concepts, which are useful for the image-level task of classification. Despite focusing on extracting more interpretable and spatially grounded concepts (Fig. 4), showing less spurious correlations, we observe in Tab. 2 that **INSIGHT yields competitive classification performance on par with the best existing, non-localized concept approach DN-CBM**.

4.3. Image captioning

We explored the performance of INSIGHT’s interpretable concept-based representation for the generative task of image captioning. We closely followed the setup of [39], appending the spatial output tokens to a language model through a transformer adapter, finetuning both the adapter and captioner on COCO [34](Karpathy splits). In Fig. 6-top we observe that INSIGHT maintains performance similar to the opaque, dense representation of the backbone, while providing an explicit concept representation, which can be edited to change the resulting captions (bottom).

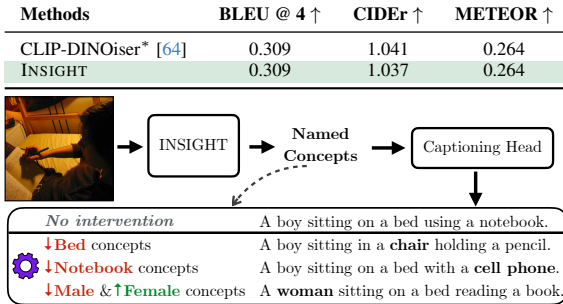


Figure 6. **INSIGHT yields competitive and steerable captioning.** (top): captioning capabilities of INSIGHT compared to its opaque backbone. (bottom): Through named concepts, INSIGHT allows for concept-level intervention, steering the image captioning.

4.4. Open Vocabulary Segmentation (OVS)

In OVS, the goal is to obtain a semantic segmentation of an image without requiring expensive data annotation limited to a specific and finite set of classes. Instead, a language-aligned vision model is used to segment images based on an open and flexible vocabulary. CLIP-DINOiser, with its semantically meaningful local features, set a strong baseline compared to existing specialized models [64].

We compare against the reported performance of prototype-based [28, 60], segmentation-specific [9, 36, 56, 58, 65, 66], as well as MaskCLIP and CLIP-DINOiser versions [64, 76] on a variety of benchmark data, including PASCAL (VOC & VOC20) [20], PASCAL (Context & Context59) [40], Coco (Object [34] & Stuff [7]), Cityscapes [15], and ADE20K [75]. We report mIoU with and without a background prompt following the established benchmarking protocol in the literature [64]. For INSIGHT, we compute the cosine similarity between the embedding of each vocabulary word with the reconstructed patch embedding of the SAE to determine the closest matching word. Through decoder weights, we moreover get an *interpretable* segmentation through linearly weighted concepts.

In Tab. 3, we observe that despite being an interpretable model, **INSIGHT performs on par with the strongest black-box baselines** in terms of mIoU, such as CLIP-DINOiser and OVDiff. It also outperforms existing specialized architectures by a wide margin across datasets. In Fig. 7 we provide curated qualitative examples of OVS on COCO-Stuff highlighting the interpretable downstream decision-making provided by INSIGHT.

5. Discussion and Conclusion

We proposed INSIGHT, a concept-based representation based on language-aligned vision encoder that represents spatially grounded and human-interpretable concepts of different granularity. As such, INSIGHT sets a new standard in the field of concept-based interpretability providing mean-

Table 3. **INSIGHT provides strong open-vocabulary semantic segmentation.** We report mIoU between segmentations and annotated parts for each dataset considering evaluation with and without a ‘background’ prompt as discussed in App. A. All results are without post-processing we took baseline results from Wysoczańska et al. [64] and rerun (*) for dataset consistency. First and second best method are **bold** and underlined, respectively.

Methods	No background prompt				w/ background			
	VOC20	C59	Stuff	City	ADE	Context	Object	VOC
<i>Build prototypes per class</i>								
ReCo [60]	57.8	22.3	14.8	21.1	11.2	19.9	15.7	25.1
OVDiff [28] ^{+(DINO & SD)}	81.7	33.7	-	-	14.9	30.1	34.8	67.1
<i>Text/image alignment training with captions</i>								
GroupViT [65]	79.7	23.4	15.3	11.1	9.2	18.7	27.5	50.4
ZeroSeg [12]	-	-	-	-	-	21.8	22.1	42.9
SegCLIP [36]	-	-	-	11.0	8.7	24.7	26.5	52.6
TCL [9]	77.5	30.3	19.6	23.1	14.9	24.3	30.4	51.2
CLIPPy [56]	-	-	-	-	13.5	-	32.0	52.2
OVSegmentor [66]	-	-	-	-	5.6	20.4	25.1	53.8
<i>Use Frozen CLIP</i>								
CLIP-DIY [63] ^{+(DINO)}	79.7	19.8	13.3	11.6	9.9	19.7	31.0	59.9
MaskCLIP [76]	61.8	25.6	17.6	25.0	14.3	22.9	16.4	32.9
MaskCLIP [76] ^{+(ref[9])}	71.9	27.4	18.6	23.0	14.9	24.0	21.6	41.3
CLIP-DINOiser* [64]	80.8	36.0	24.6	31.1	20.1	32.5	34.7	62.2
<i>Use Frozen CLIP with Interpretability</i>								
INSIGHT	77.0	32.9	22.6	27.8	18.2	28.9	31.8	59.0
INSIGHT ^{thres}	80.7	36.5	24.0	31.5	20.4	33.2	33.3	61.6
<i>Top contributing concepts (per segment)</i>								
<i>Kite Segment</i>								
Sport Kite	32.0%							
Kite String	26.9%							
Sail Boat	5.0%							
<i>Sea Segment</i>								
Body of Water	58.8%							
Tropical Beach	11.9%							
Sandy Beach	8.0%							
<i>Sand Segment</i>								
Great Sandy Desert	48.9%							
Sandy Beach	17.4%							
Body of Water	10.9%							
<i>Open-vocabulary Segmentation</i>								
Person								
Backpack								
Skateboard								
Mat								
Sail								
Sky								
Water								

Figure 7. **Explainable Open-Vocabulary Segmentation.** INSIGHT open-vocabulary segmentation (left) with concept-based explanations for each segment (right).

ingful concepts and concept names. Yet, there is still room for improvement for concept naming, as we sometimes still observe spurious correlations, which likely is inherent in the joint text and image encoder of the backbone model. We showed that the visual concepts enable interpretable decision-making across various downstream vision tasks without compromising performance compared to opaque baselines. While considering a web-scale concept representation space by learning on corresponding large datasets would be an interesting future consideration, enabling interpretable vision tokens for Vision-Language Models makes for an even more interesting future application.

References

[1] Itay Benou and Tammy Riklin Raviv. Show and Tell: Visually Explainable Deep Neural Nets via Spatially-Aware Concept Bottleneck Models. In *CVPR*, pages 30063–30072, 2025. 2, 6, 7

[2] Usha Bhalla, Alex Oesterling, Suraj Srinivas, Flavio P Calmon, and Himabindu Lakkaraju. Interpreting CLIP with Sparse Linear Concept Embeddings (SpLiCE). In *NeurIPS*, 2024. 1, 2, 21

[3] Trenton Bricken, Adly Templeton, Joshua Batson, Brian Chen, Adam Jermyn, Tom Conerly, Nick Turner, Cem Anil, Carson Denison, Amanda Askell, Robert Lasenby, Yifan Wu, Shauna Kravec, Nicholas Schiefer, Tim Maxwell, Nicholas Joseph, Zac Hatfield-Dodds, Alex Tamkin, Karina Nguyen, Brayden McLean, Josiah E Burke, Tristan Hume, Shan Carter, Tom Henighan, and Christopher Olah. Towards Monosemanticity: Decomposing Language Models With Dictionary Learning. *Transformer Circuits Thread*, 2023. 2, 4

[4] Marc Brysbaert, Amy Beth Warriner, and Victor Kuperman. Concreteness Ratings for 40 Thousand Generally Known English Word Lemmas. *Behavior Research Methods*, 46(3): 904–911, 2014. 6, 21

[5] Bart Bussmann, Patrick Leask, and Neel Nanda. BatchTopK Sparse Autoencoders. *arXiv preprint arXiv:2412.06410*, 2024. 2, 4, 19

[6] Bart Bussmann, Noa Nabeshima, Adam Karvonen, and Neel Nanda. Learning Multi-Level Features with Matryoshka Sparse Autoencoders. In *ICML*, 2025. 2

[7] Holger Caesar, Jasper Uijlings, and Vittorio Ferrari. COCO-Stuff: Thing and Stuff Classes in Context. In *CVPR*, pages 1209–1218, 2018. 7, 8, 30

[8] Mathilde Caron, Hugo Touvron, Ishan Misra, Hervé Jégou, Julien Mairal, Piotr Bojanowski, and Armand Joulin. Emerging Properties in Self-Supervised Vision Transformers. In *ICCV*, 2021. 3, 4

[9] Junbum Cha, Jonghwan Mun, and Byungseok Roh. Learning to Generate Text-Grounded Mask for Open-World Semantic Segmentation from Only Image-Text Pairs. In *CVPR*, pages 11165–11174, 2023. 6, 8

[10] Soravit Changpinyo, Piyush Sharma, Nan Ding, and Radu Soricut. Conceptual 12M: Pushing Web-Scale Image-Text Pre-Training to Recognize Long-Tail Visual Concepts. In *CVPR*, pages 3558–3568, 2021. 20

[11] Chaofan Chen, Oscar Li, Daniel Tao, Alina Barnett, Cynthia Rudin, and Jonathan K Su. This Looks Like That: Deep Learning for Interpretable Image Recognition. In *NeurIPS*, 2019. 2

[12] Jun Chen, Deyao Zhu, Guocheng Qian, Bernard Ghanem, Zhicheng Yan, Chenchen Zhu, Fanyi Xiao, Sean Chang Culatana, and Mohamed Elhoseiny. Exploring Open-Vocabulary Semantic Segmentation from CLIP Vision Encoder Distillation Only. In *ICCV*, pages 699–710, 2023. 8

[13] Zhe Chen, Jiannan Wu, Wenhui Wang, Weijie Su, Guo Chen, Sen Xing, Muyan Zhong, Qinglong Zhang, Xizhou Zhu, Lewei Lu, et al. InternVL: Scaling up Vision Foundation Models and Aligning for Generic Visual-Linguistic Tasks. In *CVPR*, pages 24185–24198, 2024. 1

[14] Mehdi Cherti, Romain Beaumont, Ross Wightman, Mitchell Wortsman, Gabriel Ilharco, Cade Gordon, Christoph Schuhmann, Ludwig Schmidt, and Jenia Jitsev. Reproducible Scaling Laws for Contrastive Language-Image Learning. In *CVPR*, pages 2818–2829, 2023. 2

[15] Marius Cordts, Mohamed Omran, Sebastian Ramos, Timo Rehfeld, Markus Enzweiler, Rodrigo Benenson, Uwe Franke, Stefan Roth, and Bernt Schiele. The Cityscapes Dataset for Semantic Urban Scene Understanding. In *CVPR*, pages 3213–3223, 2016. 8

[16] Hoagy Cunningham, Aidan Ewart, Logan Riggs, Robert Huben, and Lee Sharkey. Sparse Autoencoders Find Highly Interpretable Features in Language Models. In *ICLR*, 2024. 2

[17] Jia Deng, Wei Dong, Richard Socher, Li-Jia Li, Kai Li, and Li Fei-Fei. ImageNet: A Large-Scale Hierarchical Image Database. In *CVPR*, pages 248–255, 2009. 6

[18] Jon Donnelly, Alina Jade Barnett, and Chaofan Chen. Deformable ProtoPNet: An Interpretable Image Classifier using Deformable Prototypes. In *CVPR*, pages 10265–10275, 2022. 2

[19] Alexey Dosovitskiy, Lucas Beyer, Alexander Kolesnikov, Dirk Weissenborn, Xiaohua Zhai, Thomas Unterthiner, Mostafa Dehghani, Matthias Minderer, Georg Heigold, Sylvain Gelly, Jakob Uszkoreit, and Neil Houlsby. An Image is Worth 16x16 Words: Transformers for Image Recognition at Scale. In *ICLR*, 2021. 3

[20] Mark Everingham and John Winn. The PASCAL Visual Object Classes Challenge 2012 (VOC2012) Development Kit. *Pattern Analysis, Statistical Modelling and Computational Learning, Tech. Rep*, 8(5):2–5, 2011. 8, 30

[21] Thomas Fel, Agustin Picard, Louis Bethune, Thibaut Boissin, David Vigouroux, Julien Colin, Rémi Cadène, and Thomas Serre. CRAFT: Concept Recursive Activation Factorization for Explainability. In *CVPR*, pages 2711–2721, 2023. 2

[22] Leo Gao, Tom Dupré la Tour, Henk Tillman, Gabriel Goh, Rajan Troll, Alec Radford, Ilya Sutskever, Jan Leike, and Jeffrey Wu. Scaling and Evaluating Sparse Autoencoders. In *ICLR*, 2025. 2, 20

[23] Amirata Ghorbani, James Wexler, James Y Zou, and Been Kim. Towards Automatic Concept-Based Explanations. In *NeurIPS*, 2019. 2

[24] Ju He, Shuo Yang, Shaokang Yang, Adam Kortylewski, Xiaoding Yuan, Jie-Neng Chen, Shuai Liu, Cheng Yang, Qihang Yu, and Alan Yuille. PartImageNet: A Large, High-Quality Dataset of Parts. In *ECCV*, pages 128–145, 2022. 7

[25] Qihan Huang, Jie Song, Jingwen Hu, Haofei Zhang, Yong Wang, and Mingli Song. On the Concept Trustworthiness in Concept Bottleneck Models. In *AAAI*, pages 21161–21168, 2024. 2

[26] Gabriel Ilharco, Mitchell Wortsman, Ross Wightman, Cade Gordon, Nicholas Carlini, Rohan Taori, Achal Dave, Vaishaal Shankar, Hongseok Namkoong, John Miller, Han-

naneh Hajishirzi, Ali Farhadi, and Ludwig Schmidt. Open-CLIP, 2021. 2

[27] Chao Jia, Yinfai Yang, Ye Xia, Yi-Ting Chen, Zarana Parekh, Hieu Pham, Quoc Le, Yun-Hsuan Sung, Zhen Li, and Tom Duerig. Scaling Up Visual and Vision-Language Representation Learning with Noisy Text Supervision. In *ICML*, pages 4904–4916, 2021. 2

[28] Laurynas Karazija, Iro Laina, Andrea Vedaldi, and Christian Rupprecht. Diffusion Models for Open-Vocabulary Segmentation. In *ECCV*, pages 299–317, 2024. 6, 8

[29] Diederik P Kingma and Jimmy Ba. Adam: A Method for Stochastic Optimization. In *ICLR*, 2015. 20, 23

[30] Pang Wei Koh, Thao Nguyen, Yew Siang Tang, Stephen Mussmann, Emma Pierson, Been Kim, and Percy Liang. Concept Bottleneck Models. In *ICML*, pages 5338–5348, 2020. 2

[31] Matthew Kowal, Richard P Wildes, and Konstantinos G Derpanis. Visual Concept Connectome (VCC): Open World Concept Discovery and their Interlayer Connections in Deep Models. In *CVPR*, pages 10895–10905, 2024. 2

[32] Bo Li, Yuanhan Zhang, Dong Guo, Renrui Zhang, Feng Li, Hao Zhang, Kaichen Zhang, Peiyuan Zhang, Yanwei Li, Zizwei Liu, and Chunyuan Li. LLaVA-OneVision: Easy Visual Task Transfer. *TMLR*, 2025. 1

[33] Hyesu Lim, Jinho Choi, Jaegul Choo, and Steffen Schneider. Sparse Autoencoders Reveal Selective Remapping of Visual Concepts During Adaptation. In *ICLR*, 2025. 1, 2, 6, 7

[34] Tsung-Yi Lin, Michael Maire, Serge Belongie, James Hays, Pietro Perona, Deva Ramanan, Piotr Dollár, and C Lawrence Zitnick. Microsoft COCO: Common Objects in Context. In *ECCV*, pages 740–755, 2014. 7, 8, 23, 32

[35] Haotian Liu, Chunyuan Li, Yuheng Li, and Yong Jae Lee. Improved Baselines with Visual Instruction Tuning. In *CVPR*, pages 26296–26306, 2024. 1

[36] Huaishao Luo, Junwei Bao, Youzheng Wu, Xiaodong He, and Tianrui Li. SegCLIP: Patch Aggregation with Learnable Centers for Open-Vocabulary Semantic Segmentation. In *ICML*, pages 23033–23044, 2023. 6, 8

[37] Samuel Marks, Adam Karvonen, and Aaron Mueller. Dictionary Learning. https://github.com/saprmarks/dictionary_learning, 2024. 4

[38] Sachit Menon and Carl Vondrick. Visual Classification via Description from Large Language Models. In *ICLR*, 2023. 6, 7

[39] Ron Mokady, Amir Hertz, and Amit H Bermano. Clip-Cap: CLIP Prefix for Image Captioning. *arXiv preprint arXiv:2111.09734*, 2021. 7, 23

[40] Roozbeh Mottaghi, Xianjie Chen, Xiaobai Liu, Nam-Gyu Cho, Seong-Whan Lee, Sanja Fidler, Raquel Urtasun, and Alan Yuille. The Role of Context for Object Detection and Semantic Segmentation in the Wild. In *CVPR*, pages 891–898, 2014. 8

[41] Emiko J Muraki, Summer Abdalla, Marc Brysbaert, and Penny M Pexman. Concreteness Ratings for 62,000 English Multiword Expressions. *Behavior Research Methods*, 55(5):2522–2531, 2023. 6, 21

[42] Meike Nauta, Jörg Schlötterer, Maurice Van Keulen, and Christin Seifert. PIP-Net: Patch-based Intuitive Prototypes for Interpretable Image Classification. In *CVPR*, pages 2744–2753, 2023. 2

[43] Tuomas Oikarinen and Tsui-Wei Weng. CLIP-Dissect: Automatic Description of Neuron Representations in Deep Vision Networks. In *ICLR*, 2023. 6, 21

[44] Tuomas Oikarinen, Subhro Das, Lam M Nguyen, and Tsui-Wei Weng. Label-Free Concept Bottleneck Models. In *ICLR*, 2023. 2, 6, 7

[45] Laura O’Mahony, Vincent Andrarczyk, Henning Müller, and Mara Graziani. Disentangling Neuron Representations with Concept Vectors. In *CVPRW*, pages 3769–3774, 2023. 2

[46] Maxime Oquab, Timothée Darcet, Théo Moutakanni, Huy V. Vo, Marc Szafraniec, Vasil Khalidov, Pierre Fernandez, Daniel HAZIZA, Francisco Massa, Alaeldin El-Nouby, Mido Assran, Nicolas Ballas, Wojciech Galuba, Russell Howes, Po-Yao Huang, Shang-Wen Li, Ishan Misra, Michael Rabbat, Vasu Sharma, Gabriel Synnaeve, Hu Xu, Herve Jegou, Julien Mairal, Patrick Labatut, Armand Joulin, and Piotr Bojanowski. DINOv2: Learning Robust Visual Features without Supervision. *TMLR*, 2024. 19

[47] Konstantinos P Panousis, Dino Ienco, and Diego Marcos. Sparse Linear Concept Discovery Models. In *ICCVW*, pages 2767–2771, 2023. 6, 7

[48] Konstantinos P Panousis, Dino Ienco, and Diego Marcos. Coarse-to-Fine Concept Bottleneck Models. In *NeurIPS*, pages 105171–105199, 2024. 4, 6, 7

[49] Amin Parchami-Araghi, Sukrut Rao, Jonas Fischer, and Bernt Schiele. FaCT: Faithful Concept Traces for Explaining Neural Network Decisions. In *NeurIPS*, 2025. 2

[50] Nhi Pham, Artur Jesslen, Bernt Schiele, Adam Kortylewski, and Jonas Fischer. Interpretable 3D Neural Object Volumes for Robust Conceptual Reasoning. *arXiv preprint arXiv:2503.13429*, 2025. 13

[51] Katharina Prasse, Patrick Knab, Sascha Marton, Christian Bartelt, and Margret Keuper. DCBM: Data-Efficient Visual Concept Bottleneck Models. In *ICML*, 2025. 6, 7

[52] Alec Radford, Jeff Wu, Rewon Child, David Luan, Dario Amodei, and Ilya Sutskever. Language Models are Unsupervised Multitask Learners. 2019. 23

[53] Alec Radford, Jong Wook Kim, Chris Hallacy, Aditya Ramesh, Gabriel Goh, Sandhini Agarwal, Girish Sastry, Amanda Askell, Pamela Mishkin, Jack Clark, et al. Learning Transferable Visual Models from Natural Language Supervision. In *ICML*, pages 8748–8763, 2021. 1, 2, 3

[54] Senthooran Rajamanoharan, Arthur Conmy, Lewis Smith, Tom Lieberum, Vikrant Varma, János Kramár, Rohin Shah, and Neel Nanda. Improving Sparse Decomposition of Language Model Activations with Gated Sparse Autoencoders. In *NeurIPS*, 2024. 2

[55] Senthooran Rajamanoharan, Tom Lieberum, Nicolas Sonnerat, Arthur Conmy, Vikrant Varma, János Kramár, and Neel Nanda. Jumping Ahead: Improving Reconstruction Fidelity with JumpReLU Sparse Autoencoders. *arXiv preprint arXiv:2407.14435*, 2024. 2

[56] Kanchana Ranasinghe, Brandon McKinzie, Sachin Ravi, Yinfei Yang, Alexander Toshev, and Jonathon Shlens. Perceptual Grouping in Contrastive Vision-Language Models. In *ICCV*, pages 5571–5584, 2023. 6, 8

[57] Sukrut Rao, Sweta Mahajan, Moritz Böhle, and Bernt Schiele. Discover-then-Name: Task-Agnostic Concept Bottlenecks via Automated Concept Discovery. In *ECCV*, 2024. 1, 2, 5, 6, 7, 21

[58] Pitchaporn Rewatbowornwong, Nattanat Chathee, Ekapol Chuangsuvanich, and Supasorn Suwajanakorn. Zero-Guidance Segmentation Using Zero Segment Labels. In *ICCV*, pages 1162–1172, 2023. 6, 8

[59] Olga Russakovsky, Jia Deng, Hao Su, Jonathan Krause, Sanjeev Satheesh, Sean Ma, Zhiheng Huang, Andrej Karpathy, Aditya Khosla, Michael Bernstein, Alexander C. Berg, and Li Fei-Fei. ImageNet Large Scale Visual Recognition Challenge. *IJCV*, 115(3):211–252, 2015. 7, 19

[60] Gyungin Shin, Weidi Xie, and Samuel Albanie. ReCo: Retrieve and Co-segment for Zero-shot Transfer. *NeurIPS*, 35: 33754–33767, 2022. 6, 8

[61] Ao Sun, Yuanyuan Yuan, Pingchuan Ma, and Shuai Wang. Eliminating Information Leakage in Hard Concept Bottleneck Models with Supervised, Hierarchical Concept Learning. *arXiv preprint arXiv:2402.05945*, 2024. 4

[62] Michael Tschanne, Alexey Gritsenko, Xiao Wang, Muhammad Ferjad Naeem, Ibrahim Alabdulmohsin, Nikhil Parthasarathy, Talfan Evans, Lucas Beyer, Ye Xia, Basil Mustafa, et al. SigLIP 2: Multilingual Vision-Language Encoders with Improved Semantic Understanding, Localization, and Dense Features. *arXiv preprint arXiv:2502.14786*, 2025. 1, 2

[63] Monika Wysoczańska, Michaël Ramamonjisoa, Tomasz Trzciński, and Oriane Siméoni. CLIP-DIY: CLIP Dense Inference Yields Open-Vocabulary Semantic Segmentation For-Free. In *WACV*, pages 1403–1413, 2024. 4, 8

[64] Monika Wysoczańska, Oriane Siméoni, Michaël Ramamonjisoa, Andrei Bursuc, Tomasz Trzciński, and Patrick Pérez. CLIP-DINOiser: Teaching CLIP a Few DINO Tricks for Open-Vocabulary Semantic Segmentation. In *ECCV*, pages 320–337, 2024. 2, 3, 8, 19

[65] Jiarui Xu, Shalini De Mello, Sifei Liu, Wonmin Byeon, Thomas Breuel, Jan Kautz, and Xiaolong Wang. GroupViT: Semantic Segmentation Emerges from Text Supervision. In *CVPR*, pages 18134–18144, 2022. 6, 8

[66] Jilan Xu, Junlin Hou, Yuejie Zhang, Rui Feng, Yi Wang, Yu Qiao, and Weidi Xie. Learning Open-Vocabulary Semantic Segmentation Models from Natural Language Supervision. In *CVPR*, pages 2935–2944, 2023. 6, 8

[67] Mengqi Xue, Qihan Huang, Haofei Zhang, Lechao Cheng, Jie Song, Minghui Wu, and Mingli Song. ProtoPFormer: Concentrating on Prototypical Parts in Vision Transformers for Interpretable Image Recognition. In *IJCAI*, 2022. 2

[68] Yue Yang, Artemis Panagopoulou, Shenghao Zhou, Daniel Jin, Chris Callison-Burch, and Mark Yatskar. Language in a Bottle: Language Model Guided Concept Bottlenecks for Interpretable Image Classification. In *CVPR*, pages 19187–19197, 2023. 6, 7

[69] Christine Ye, Charles O’Neill, John F Wu, and Kartheik G. Iyer. Sparse Autoencoders for Dense Text Embeddings Reveal Hierarchical Feature Sub-Structure. In *NeurIPS Workshop on Scientific Methods for Understanding Deep Learning*, 2024. 5

[70] Jiahui Yu, Zirui Wang, Vijay Vasudevan, Legg Yeung, Mojtaba Seyedhosseini, and Yonghui Wu. CoCa: Contrastive Captioners are Image-Text Foundation Models. *TMLR*, 2022. 2

[71] Mert Yuksekgonul, Maggie Wang, and James Zou. Post-hoc Concept Bottleneck Models. In *ICLR*, 2023. 2

[72] Vladimir Zaigrajew, Hubert Baniecki, and Przemysław Biecek. Interpreting CLIP with Hierarchical Sparse Autoencoders. In *ICML*, 2025. 1, 2, 4, 6, 7, 21

[73] Xiaohua Zhai, Basil Mustafa, Alexander Kolesnikov, and Lucas Beyer. Sigmoid Loss for Language Image Pre-Training. In *ICCV*, pages 11975–11986, 2023. 1, 2

[74] Bolei Zhou, Agata Lapedriza, Aditya Khosla, Aude Oliva, and Antonio Torralba. Places: A 10 million Image Database for Scene Recognition. *IEEE TPAMI*, 2017. 6, 7

[75] Bolei Zhou, Hang Zhao, Xavier Puig, Tete Xiao, Sanja Fidler, Adela Barriuso, and Antonio Torralba. Semantic Understanding of Scenes through the ADE20k Dataset. *IJCV*, 127(3):302–321, 2019. 8, 30

[76] Chong Zhou, Chen Change Loy, and Bo Dai. Extract Free Dense Labels from CLIP. In *ECCV*, pages 696–712, 2022. 3, 8

INSIGHT: Interpretable Semantic Hierarchies in Vision-Language Encoders

Appendix

In this supplement to our work on interpretable semantic hierarchies (INSIGHT), we provide additional details on model training, experimental metrics, user study design and analysis, and additional qualitative results. In particular, Appendix A is dedicated to experimental details, where we formally define the interpretability metrics reported in Table 1 in the main manuscript, and discuss details of how we conducted the user study in Amazon MTurk, provide screenshots of its interface, and provide additional analysis of results stratified by concept activations frequency and results for concept naming quality.

In Appendix B, we provide all necessary technical details to reproduce our results, including formal definitions of the CLIP-DINOiser trick, its training objective, how Matryoshka SAEs were trained including the choice of hyperparameters, and formal details on family discovery and concept naming used in INSIGHT. Lastly we provide training details for the classification and image captioning tasks, the Open Vocabulary Segmentation task is already addressed in the main manuscript.

In Appendix C, we provide additional qualitative results spanning all aspects of INSIGHT, including concept relations, spatial grounding of concepts, and downstream tasks. We *highly encourage the reader to take a look at these results*. These are curated examples to show the diversity and granularity of concepts as well as family relations that INSIGHT can find, but also to show the subtle limitations when it comes to naming fine-grained concepts. The following table of contents allows for fast access to the individual sections.

(A) Experimental Details	13
(A.1) Interpretability Metrics	
(A.2) User Study	
(B) Training of INSIGHT	19
(B.1) CLIP-DINOiser Training	
(B.2) Matryoshka SAE Training	
(B.3) Family Discovery	
(B.4) Concept Naming	
(B.5) Probing for Classification	
(B.6) Image Captioning	
(C) Additional Results	24
(C.1) Concept Families	
(C.2) Random Concept Visualization	
(C.3) Interpretable Classification	
(C.4) Interpretable Open Vocabulary Segmentation	
(C.5) Steerable Captioning	

A. Experimental Details

A.1. Interpretability Metrics

To quantitatively evaluate the locality of our discovered concepts, we compare INSIGHT against three existing approaches: DN-CBM (data-driven global concepts), MSAE (data-driven global concepts), PatchSAE (data-driven local concepts), and SALF-CBM (predefined local concepts). Given the substantial differences in concept vocabularies, sparsity patterns, and spatial representations across these methods, we develop a comprehensive evaluation framework with five complementary metrics inspired by Pham et al. [50], adapted to enable fair comparison across diverse concept discovery approaches and diverse concept sets.

A.1.1. Locality Metric

This metric measures how well concept spatial activations match human-annotated segments: Let $\mathbb{1}_c(i, j)$ and $\mathbb{1}_l(i, j)$ denote binary indicators of whether concept c or label l is active at pixel (i, j) . For a concept c and label l on image x :

$$\text{IoU}_{c,l}(x) = \frac{\sum_{i,j} \mathbb{1}_c(i, j) \cdot \mathbb{1}_l(i, j)}{\sum_{i,j} \mathbb{1}_{c,l}(i, j)}. \quad (\text{A.1})$$

The overall Locality score is:

$$\text{Locality} = \frac{1}{|L_x|} \sum_{l \in L_x} \frac{1}{|I|} \sum_{x \in I} \max_{c \in C} \text{IoU}_{c,l}(x). \quad (\text{A.2})$$

where I is the set of images and L_x is the set of labels present in image x . For each image, we compute per human-annotated label the maximum IoU over all concepts and then average across images and labels.

A.1.2. Consistency Metric

This metric evaluates whether concepts reliably capture the same semantic regions across images:

$$\text{Consistency} = \frac{1}{|L|} \sum_{l \in L} \max_{c \in C} \frac{1}{|I_l^c|} \sum_{i \in I_l^c} \text{IoU}_{c,l}(i), \quad (\text{A.3})$$

where I_l^c is the set of images where both concept c and label l are present. For each concept-label pair, we compute the mean IoU across all images where both the concept and label are present, then take the maximum over concepts for each label.

A.1.3. Impurity Metric

This metric measures the spatial focus of concepts within single labels:

$$\text{Impurity} = \frac{1}{|C_{\text{active}}|} \sum_{c \in C_{\text{active}}} \frac{1}{|I_c|} \sum_{i \in I_c} H(p_i^c), \quad (\text{A.4})$$

where C_{active} is the set of concepts that activate in at least 5 images for PartImageNet and 20 images for COCO-Stuff, I_c is the set of images where concept c is active, and $H(p_i^c)$ is the entropy of the normalized activation distribution of concept c across all labels (including background) in image i :

$$H(p_i^c) = - \sum_{l \in L \cup \{\text{bg}\}} p_i^{c,l} \log p_i^{c,l}, \quad (\text{A.5})$$

where $p_i^{c,l} = \frac{\sum_{\text{pixels} \in S_i^l} B_i^c}{\sum_{\text{all pixels}} B_i^c}$. For each concept, we compute the entropy of its activations across all human-annotated labels (including background), then average over the images. For the final score we average over all concepts that activate at least in the specified number of images. Lower values indicate concepts that concentrate within specific semantic regions rather than spreading across multiple labels. Note that the metric is on a log scale.

A.2. User Study

To evaluate concept quality from a human perspective, we performed a large scale user study. We describe the setup in Sec. A.2.1, and provide additional analysis of the results in Sec. A.2.2.

A.2.1. Study Setup

We conducted a study in Amazon Mechanical Turk comprising three tasks: evaluating (1) concept consistency, (2) concept naming quality, and (3) concept relationship quality. Task 1 and task 2 consist of 1000 questions each, while task 3 contains 1100 questions. Each question is supposed to be labeled by five annotators. For each task, groups of 20 questions are created to form ‘Human Intelligence Tasks’ (HITs) in Amazon Mechanical Turk. A HIT is the smallest task unit an annotator can complete, *i.e.* for any task an annotator reads the instructions and completes 20 questions (and might optionally continue completing more HITs). To help annotation quality, we use annotators located in the US, with at least 10000 approved HITs, and with at least a 98% HIT approval rate. We pay annotators \$2.00 per completed HIT (*i.e.* \$0.10 per question), with an estimated time of five minutes for solving a HIT. All HITs inform annotators on how their responses will be used and require them to provide consent. In the following, we provide additional details about each task.

Task 1: Concept consistency. In this task we ask annotators to rate the consistency of concepts from INSIGHT on a five-point scale. Each question consists of the top five activating images and corresponding concept locality maps for an INSIGHT SAE latent (a concept). We call concept locality maps “focus regions” to ensure easier understanding for layman. We bin latents into five equi-height bins based on frequency of their activation across images, and sample uniformly from each bin. We sample 908 concepts and additionally create 92 ‘random’ questions for control, *i.e.* questions where the 5 images and their focus regions are drawn iid from all SAE latents. For more details and an example, see Fig. A1.

Task 2: Concept naming quality. In this task we ask annotators to provide a one to two word label for an INSIGHT concept. Each question consists of the top five activating images and corresponding concept locality maps for an INSIGHT SAE latent. We follow the same binning based on activation frequency as above and sample equally from each bin. We sample 908 concepts and additionally create 92 ‘random’ questions for control, *i.e.* questions where the 5 images and their focus regions are drawn iid from all SAE latents. If no name can be provided, annotators have the option to answer ‘NA’. For more details and an example, see Fig. A2.

Task 3: Concept relationship quality. In this task we ask annotators to rate a given relationship between two concepts from INSIGHT on a five-point scale, and we use this task to evaluate the quality of family relationships from INSIGHT. Each question consists of the top three activating images and corresponding concept locality maps for two SAE latents from INSIGHT. We bin latents into five bins based on frequency of their activation across images, and sample equally from each bin. We sample 990 concept pairs that correspond to edges from the INSIGHT concept families and additionally create 110 ‘random’ relations across all concepts that do not have a real relation in our graph \mathcal{G} for control. For more details and an example, see Fig. A3.

A.2.2. Results

Quality Filtering. We apply three types of filtering to obtain consensual and higher quality results. For all tasks, we exclude those participants that did not answer the box asking for consent to being a participant. For task 1 and task 3, respectively, we filter out those participants that gave a score > 3 for one of the random control questions, as they likely did not understand the task or answered randomly. For task 2, we exclude those participants that gave NA as label for almost every question. This leaves us with scores of 152 unique participants for task 1, 107 for task 2, and 158 for task 3.

Statistics on Concept Naming Quality. We provide the results of our study on naming quality in Fig. A4a, comparing the consistency scores given by users to top-5 images of an actual concept against 5 images randomly drawn from different concepts. Measuring cosine similarity between SentenceBERT (SBERT) embeddings of user-provided names against concept naming of INSIGHT or random names, we observe a stark and statistically significant ($p < 2.22e - 16$ Wilcoxon rank-sum test) difference between our assigned names versus randomly drawn names from our set of concept names discovered by our method. This provides evidence that INSIGHT assigns names that meaningfully align with human labeling.

Statistics Stratified by Activation Frequency. To investigate how activation frequency of a concept, which is a reflection of its generality and correlates with the Matryoshka shells, impacts human interpretability, we investigate how stratification by activation frequency bins impacts study results. For both, task 1 and 2 (see Fig. A4), we observe that results look largely consistent across bins with slight improvements in scores for less frequently activated bins. In other words, we see a slight (negative) correlation between activation frequency and scores. This is to be expected, as frequently activated,

Consistency Rating (5-point scale)

- This task has **20 questions** and takes about **5 minutes** (~15 s per question).
- Each question shows a **focus regions** from **five images** on top, and the images they were taken from at the bottom.
- Rate whether the focus regions across the five images indicate a **consistent, human-understandable theme, object, or concept**, using the 5-point scale below.
- Consistent** means the focus regions share a common theme or notion, for example same type of object (all flowers), OR same colours (all blue regions), OR same parts (all wheels), etc.
- Not consistent** means that the focus regions do not share a common theme, object, or concept.
- Use the examples below to guide your ratings.

This study aims at evaluating and developing more transparent machine-learned models. To participate, you must be at least 18 years old. Your answers are anonymized and gathered for research purposes. Your participation in this study is voluntary and you can withdraw from it at any time. Only subjects that finish the study are compensated.

By checking this box you confirm that you read the information above and agree to participate in this research study.

5-point scale

- 5 – Fully consistent (BEST):** clear concept across all five.
- 4 – Mostly:** strong relation but with minor issues.
- 3 – Somewhat:** mixed.
- 2 – Slightly:** weak/occasional relation.
- 1 – Not consistent (WORST):** no shared concept.

Select one rating (1-5) for each image: 5 – FULLY consistent (BEST) / 4 – Mostly / 3 – Somewhat / 2 – Slightly / 1 – NOT consistent (WORST)

Question 1

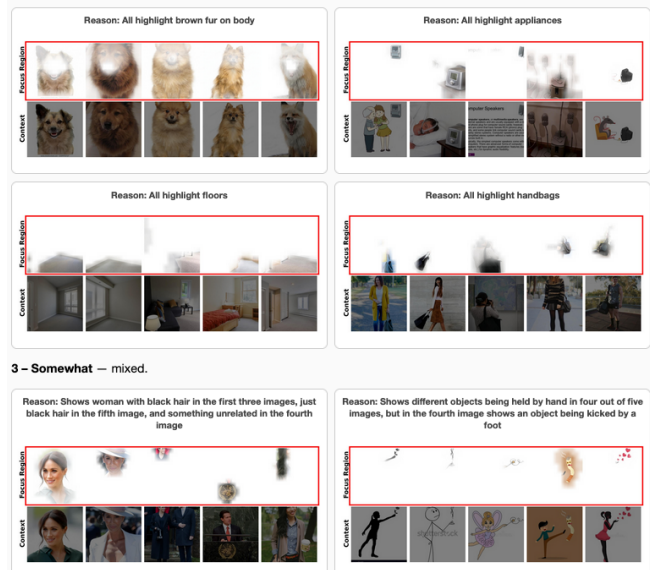
Focus Region	Context

5 - FULLY consistent (BEST) 4 - Mostly 3 - Somewhat 2 - Slightly 1 - NOT consistent (WORST)

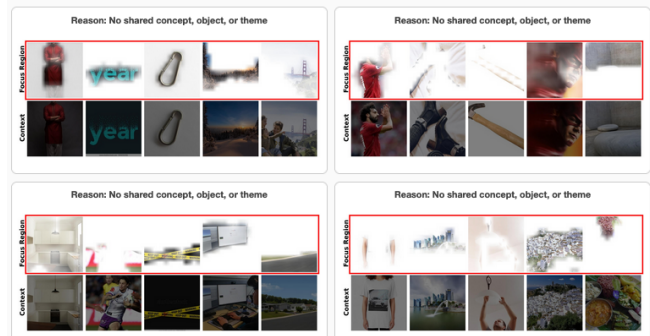
(a) Top: Task instructions. Bottom: A question in the task.

Examples

5 – Fully consistent — clear concept across all five.



1 – Not consistent — no shared concept.



(b) Examples provided after the instructions to guide annotators.

Figure A1. **Task 1 instructions and an example question.** See Sec. A.2.1 for details on the study setup.

general concepts activate on more diverse images, often capture more abstract or high-level concepts that are seemingly less consistent compared to the more specific concepts, given the larger variation in images. Similarly, it is harder to identify a clear and crisp label for a high-level concept compared to a highly specific one.

Concept Name: 1–2 Word Label

- This task has **20 questions** and takes about **5 minutes** (~15 s per question).
- Each question shows **focus regions** from **five images** on top, and the images they were taken from at the bottom.
- **Type a 1–2 word label that best describes the common theme** in the focus regions. If there is **no evident theme**, type **NA**.

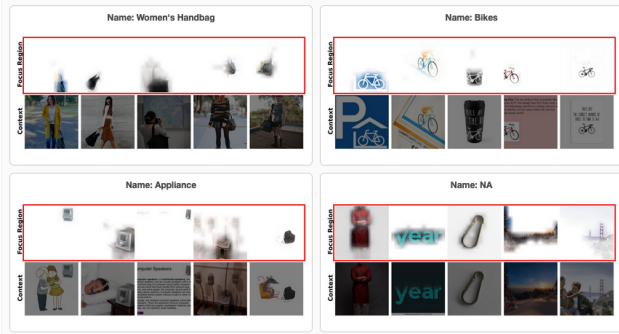
This study aims at evaluating and developing more transparent machine-learned models. To participate, you must be at least 18 years old. Your answers are anonymized and gathered for research purposes. Your participation in this study is voluntary and you can withdraw from it at any time. Only subjects that finish the study are compensated.

By checking this box you confirm that you read the information above and agree to participate in this research study.

How to label

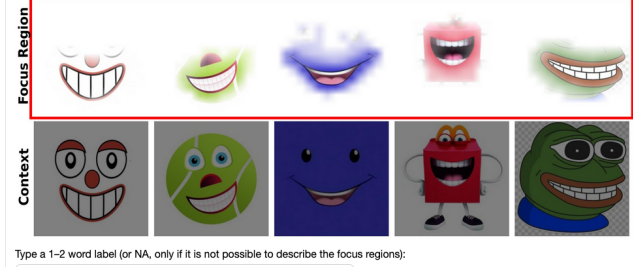
- Use short, generic words (e.g., *number*, *face*, *metal pipe*, *fur*).
- Avoid sentences; **1–2 words only**. If unsure, type **NA**.
- Look for what the highlights have in common across all five.

Examples



(a) Task instructions along with examples to guide annotators.

Question 11



(b) A question in the task.

Figure A2. **Task 2 instructions and an example question.** See Sec. A.2.1 for details on the study setup.

Rate how well two concepts are related (5-point scale)

- This task has **20 questions** and takes about **5 minutes** (~15 s per question).
- Each question shows two groups of images **A** and **B**, each of which is given by **focus regions** at the top, and images they were taken from at the bottom.
- Using the 5-point scale below, rate how **related** the **focus regions** of **A** and **B** are.
- Examples of relationships include, but are not limited to, one group showing a concept that is a part of the other (e.g. dog and dog tail), or one group showing a concept being a specialized instance of the other (animal and dog).
- The order of the two groups does not matter.
- Use the examples below to guide your ratings.

This study aims at evaluating and developing more transparent machine-learned models. To participate, you must be at least 18 years old. Your answers are anonymized and gathered for research purposes. Your participation in this study is voluntary and you can withdraw from it at any time. Only subjects that finish the study are compensated.

By checking this box you confirm that you read the information above and agree to participate in this research study.

5-point scale

- 5 – Fully related (BEST)
- 4 – Mostly related
- 3 – Partly related
- 2 – Slightly related
- 1 – Not at all related (WORST)

Select one rating (1–5) for each image: 5 - FULLY related (BEST) / 4 - Mostly related / 3 - Partly related / 2 - Slightly related / 1 - NOT AT ALL related (WORST)

Question 1

A



Focus Region

Context

B



Focus Region

Context

5 - FULLY related (BEST)

4 - Mostly related

3 - Partly related

2 - Slightly related

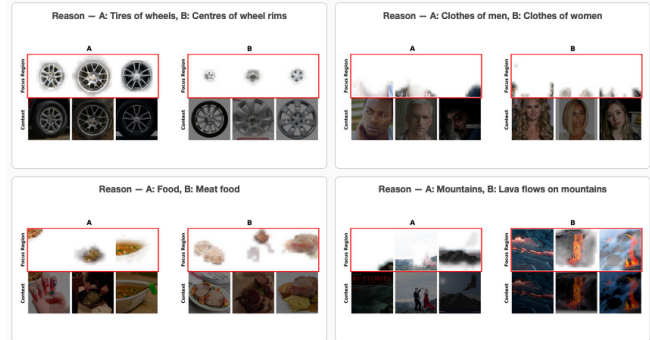
1 - NOT AT ALL related (WORST)

(a) Top: Task instructions. Bottom: A question in the task.

Figure A3. **Task 3 instructions and an example question.** See Sec. A.2.1 for details on the study setup.

Examples

5 – Fully related



3 – Partly related



(b) Examples provided after the instructions to guide annotators.

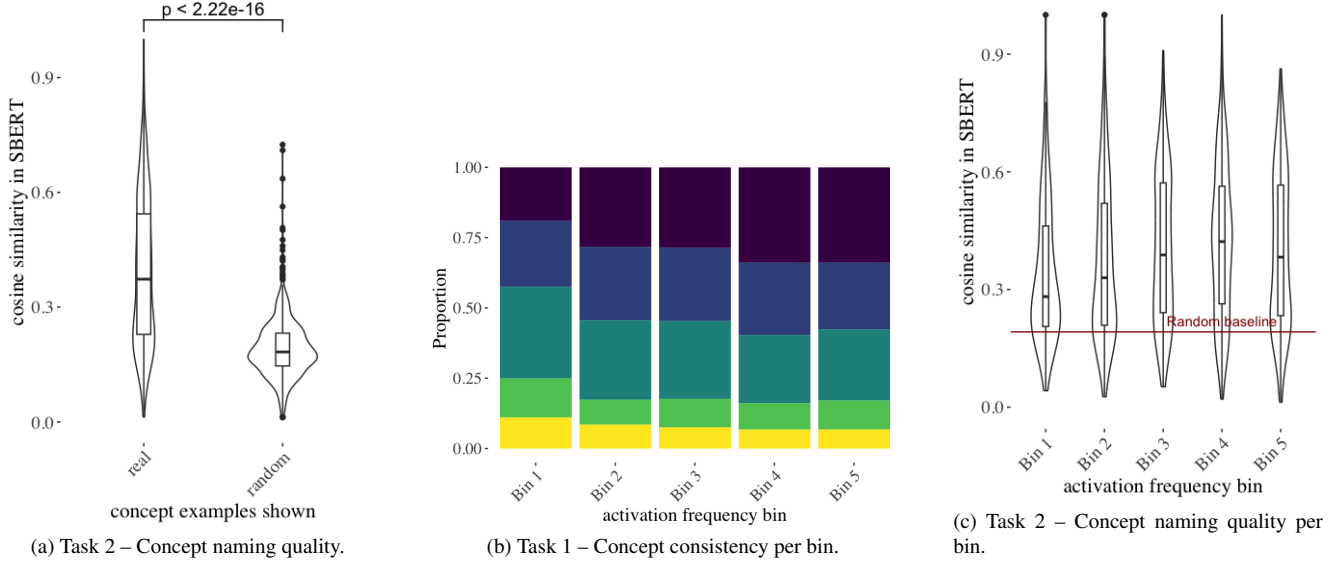


Figure A4. **Additional User Study Results.** We provide (a) concept naming quality, measured as average cosine similarity between SBERT embeddings of INSIGHT concept naming and user-provided labels versus random names, p-value based on Wilcoxon rank-sum test, (b) concept consistency partitioned into concept activation frequency bins, with scores 1 (no consistency, yellow) to 5 (full consistency, purple) and (c) concept naming quality partitioned into concept activation frequency bins, red line indicates mean random similarity.

B. Training of INSIGHT

This section provides detailed training procedures for all components of INSIGHT. We follow the notation established in the main paper (Sec. 3), recap the CLIP-DINOiser training, with a focus on the lightweight convolution, in Sec. B.1, discuss SAE training in Sec. B.2, family discover in Sec. B.3, concept naming in Sec. B.4, classifier training in Sec. B.5, and training for image captioning in Sec. B.6.

B.1. CLIP-DINOiser Training

Following Wysoczańska et al. [64], we train a lightweight 3×3 convolutional layer $g : \mathbb{R}^d \rightarrow \mathbb{R}^{d'}$ with $d = 512$ and $d' = 64$ to approximate DINO affinity patterns from CLIP patch tokens.

Training objective. The convolution g is trained to predict binarized DINOv2 [46] affinities. Given patch tokens X from the final CLIP layer L , we compute predicted affinities as in Eq. (2) of the main paper:

$$A^\phi = \frac{g(\phi^L(X))}{\|g(\phi^L(X))\|} \otimes \left(\frac{g(\phi^L(X))}{\|g(\phi^L(X))\|} \right)^T. \quad (\text{B.1})$$

The training loss is binary cross-entropy between A^ϕ and binarized DINO affinities $D = A^\xi > \gamma$:

$$\mathcal{L}^C = \sum_{p=1}^N [D_p \log A_p^\phi + (1 - D_p) \log(1 - A_p^\phi)], \quad (\text{B.2})$$

where $\gamma = 0.2$ is the binarization threshold.

Training setup. We train on 1,000 randomly sampled images from Imagenet [59] under learning rate of $5e-5$ with batch size of 16 for 100 epochs. The CLIP ViT-B/16 backbone ϕ and DINO ViT-B/16 remain frozen throughout training.

B.2. Matryoshka SAE Training

We train hierarchical Matryoshka Sparse Autoencoders with BatchTopK sparsity [5] on DINOised patch features F^+ extracted as described in Sec. 3.1 of the main paper.

Architecture. The SAE consists of encoder $\pi : \mathbb{R}^d \rightarrow \mathbb{R}^m$ and decoder $\pi^{-1} : \mathbb{R}^m \rightarrow \mathbb{R}^d$ where $d = 512$ is the CLIP embedding dimension and $m = 8192$ is the number of concepts (expansion factor of 16).

For a patch embedding $F_p^+ \in \mathbb{R}^d$, the encoder computes pre-activation features:

$$z_{\text{pre}} = W_{\text{enc}}^T (F_p^+ - b_{\text{dec}}) + b_{\text{enc}} \quad (\text{B.3})$$

where $W_{\text{enc}} \in \mathbb{R}^{d \times m}$ are encoder weights, $b_{\text{enc}} \in \mathbb{R}^m$ is the encoder bias, and $b_{\text{dec}} \in \mathbb{R}^d$ is the decoder bias (shared with the decoder).

BatchTopK sparsity. Following Bussmann et al. [5], we apply batch-level top- k activation, which retains exactly $B \cdot k$ neurons across a batch of size B :

$$z = \pi(F_p^+) = \text{ReLU}(\text{BatchTopK}(z_{\text{pre}})) \quad (\text{B.4})$$

where BatchTopK sets all but the top $B \cdot k$ pre-activations to zero across the entire batch. We use $k = 12$, meaning the SAE activates 12 concepts per patch on average.

Matryoshka structure. Following Sec. 3.2 of the main paper, we organize the $m = 8192$ concepts into six hierarchical groups with size ratios $[0.008, 0.03, 0.06, 0.12, 0.24, 0.543]$. Let $C = [1 \dots m]$ be the index set and $l_j \in C$ the index defining Matryoshka shell j . The reconstruction loss from the main paper is:

$$\mathcal{L}_{\text{rec}}(F_p^+) = \sum_j \cdot \left\| \pi^{-1}(\pi(F_p^+)[1 : l_j]) - F_p^+ \right\|_2^2 \quad (\text{B.5})$$

where $\pi(F_p)[1 : l_j]$ sets all activations after index l_j to zero.

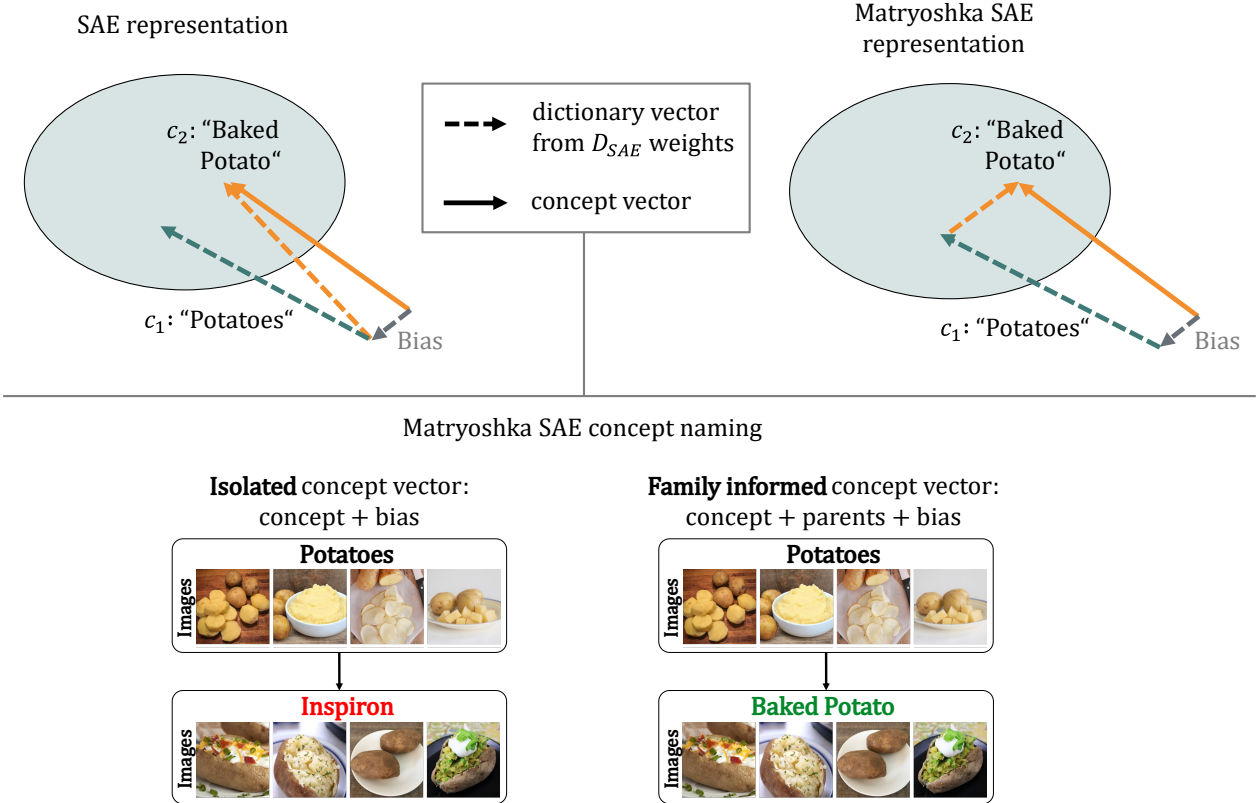


Figure B1. **Adapted concept vector reconstruction.** In standard SAE representations, the dictionary vector of a concept given by the SAE decoder weights of the corresponding neuron can be used as concept vector (left) for finding a closest text label. In Matryoshka SAEs, dictionary vectors in different Matryoshka shells are residual by design, hence concept vectors are the sum of all dictionary vectors of super-concepts (right). These super-concept relationships are all descendants of the target concepts in our relationship graph (Sec. 3.3). This is necessary to obtain meaningful text labels for fine-grained concepts (bottom left versus bottom right).

Auxiliary loss for dead features. To recover neurons that haven't activated recently (last 10,000,000 samples), we add an auxiliary loss [22]:

$$\mathcal{L}_{\text{aux}} = \frac{\|r - W_{\text{dec}}^T z_{\text{dead}}\|_2^2}{\|r - \bar{r}\|_2^2} \quad (\text{B.6})$$

where $r = F_p^+ - \pi^{-1}(\pi(F_p))$ is the reconstruction residual, \bar{r} is the batch-mean residual, and z_{dead} are activations for dead features only. Hence the total loss is

$$\mathcal{L}_{\text{total}} = \mathcal{L}_{\text{rec}} + \alpha_{\text{aux}} \cdot \mathcal{L}_{\text{aux}} \quad (\text{B.7})$$

with $\alpha_{\text{aux}} = \frac{1}{32}$.

Training setup. We train on all DINOised patch embeddings extracted from CC12M [10]. Each image yields $N = 196$ patches (14×14 grid), providing approximately 2 billion training samples. We use Adam optimizer [29], with learning rate of $1e-4$. We set the batch size to 16,268 from 83 images and train for 3 epochs. We keep 10% of the patches as held-out validation set. Our training converges within 3 epochs with fraction of variance explained reaching approximately 73% and number of dead features dropping below 10.

B.3. Family Discovery

After SAE training, we discover concept relationships by analyzing patch-level co-occurrence patterns as described in Sec. 3.3 of the main paper.

Confidence matrix computation. For each concept pair $(c_j, c_{j'})$, we compute the weighted confidence matrix D as defined in the main paper:

$$D_{j,j'} = \frac{\sum_i \mathbb{1}_{j'j} A_{ji}}{\sum_i A_{ji}}, \quad (\text{B.8})$$

where $\mathbb{1}_{ji}$ is a binary indicator if concept c_j is activated in patch i and A_{ji} is the activation strength of concept c_j at patch i . The sum is over all patches of all training images in CC12M.

Graph construction. We construct the family graph $\mathcal{G} = (V, E)$ where:

- $V = C$ (vertices are concepts)
- $(c_j, c_{j'}) \in E$ if $D_{j,j'} \geq 0.75$

We then invert all edge directions to obtain parent \rightarrow child relationships (general \rightarrow specific concepts), as described in Sec. 3.3.

B.4. Concept Naming

Following Sec. 3.4 of the main paper, we assign concept names using family-informed vector reconstruction.

Vector reconstruction. For fine-grained concepts in later Matryoshka groups, dictionary vectors π_i^{-1} alone are insufficient as they encode residuals from parent concepts (see Fig. B1). We reconstruct family-informed concept vectors:

$$v_{c_i} = b + \alpha \cdot w_{ii} \cdot \pi_i^{-1} + \sum_{a \in \mathcal{G}, a \rightarrow i} D_{ia} \cdot w_{ia} \cdot \pi_a^{-1}, \quad (\text{B.9})$$

where:

- b is the SAE decoder bias b_{dec}
- π_i^{-1} is the dictionary vector (decoder weights for concept i)
- $a \rightarrow i$ denotes parent a of concept i in graph \mathcal{G}
- D_{ia} is the confidence from the co-occurrence matrix
- w_{ia} is the mean activation of concept a in the top-30 most activating patches of concept i
- $\alpha = 1.33$ is an empirically chosen coefficient to strengthen the concept's own direction in the embedding space

The coefficient $\alpha > 1$ ensures concept i 's dictionary vector receives stronger weight than parent vectors, maintaining specificity while incorporating parent context.

Vocabulary matching. Given reconstructed vector v_{c_i} , we assign names as in Sec. 3.4:

$$l_i = \text{argmax}_{v \in V} \cos(v_{c_i}, \mathcal{T}(v)), \quad (\text{B.10})$$

where \mathcal{T} is the CLIP text encoder and V is our vocabulary.

As such, we get meaningful labels across concepts of different granularity. This assumes that the query vocabulary V is rich enough. We found that vocabularies used in concurrent works [57, 72] are often too limited for fine-grained concept labeling.

Vocabulary construction. To ensure comprehensive coverage, we construct our vocabulary by combining multiple resources. Concretely, our vocabulary includes (1) Common words as the 20k most frequent English words from [43], (2) a filtered 40k-word dataset from Brysbaert et al. [4], in which each word is annotated with a concreteness score between 1 (abstract) and 5 (highly concrete) and we retain only words with a mean concreteness above 2.5 as concreteness correlates strongly with imageability, (3) multi-word expressions from Muraki et al. [41], filtering with a concreteness threshold of 2.0, and (4) LAION expressions following the approach of Bhalla et al. [2], extracting the 40k most frequent uni-words from LAION-400M, filtering NSFW captions using the given NSFW flag. Furthermore, we include the bi-words extracted by Bhalla et al. [2]. After gathering all resources, we merge them into a single comprehensive candidate vocabulary that balances coverage, concreteness, and fine-grained expressivity and provides a good resource for meaningful concept naming.

Vocabulary Templates. To improve labeling accuracy, we use sentence templates to encode the query vocabulary. However using the standard Zero-shot templates biases the labeling toward nouns, as CLIP’s text encoder is sensitive to grammatical context. To allow concepts to be labeled by nouns, verbs, or adjectives, we introduce three distinct template sets, one for each part of speech. Each set contains ten abstract templates $\{\tau_k^{(p)}\}_{k=1}^{10}$, where $p \in \{\text{noun, verb, adj}\}$. Example templates include patterns such as “a photo of a {}” (noun), “a photo of someone {}” (verb), or “something that is {}” (adjective). We deliberately avoid overly specific templates to prevent unintentionally biasing the meaning of vocabulary items.

Given a vocabulary item $v \in V$, we generate its template-conditioned embeddings by applying the CLIP text encoder \mathcal{T} to each templated prompt:

$$E_p(v) = \frac{1}{10} \sum_{k=1}^{10} \frac{\mathcal{T}(\tau_k^{(p)}(v))}{\|\mathcal{T}(\tau_k^{(p)}(v))\|_2}, \quad p \in \{\text{noun, verb, adj}\}. \quad (\text{B.11})$$

Each $E_p(v)$ is then normalized to unit length. For every concept vector v_{c_i} , we compute the cosine similarity to all template-conditioned embeddings:

$$s_i(v) = \max_{p \in \{\text{noun, verb, adj}\}} \cos(v_{c_i}, E_p(v)). \quad (\text{B.12})$$

Finally, we assign the vocabulary label that achieves the highest similarity:

$$l_i = \arg \max_{v \in V} s_i(v). \quad (\text{B.13})$$

This template-based strategy enables each concept to select the grammatical form that best fits its semantics, yielding more accurate and fine-grained names than noun-only matching.

B.5. Linear Probe for Classification

For downstream classification tasks, we train a linear probe on image-level concept activations while keeping all other components frozen (i.e., not fine-tuning).

Concept aggregation. We aggregate patch-level concept activations to image-level by combining max pooling and mean pooling:

$$\hat{c}_i^{\max} = \max_{p \in \{1, \dots, N\}} z_{i,p}, \quad \hat{c}_i^{\text{mean}} = \frac{1}{N} \sum_{p=1}^N z_{i,p}, \quad (\text{B.14})$$

and form the final image-level concept vector by concatenating both:

$$\hat{c}_i = [\hat{c}_i^{\max}; \parallel; \hat{c}_i^{\text{mean}}], \quad (\text{B.15})$$

where $z_{i,p} \in \mathbb{R}^m$ are the sparse concept activations given by our SAE concept mapping (see Eq.B.4) for patch p of image i , and $N = 196$ is the number of patches. We find that using only max-pooled concepts yields comparable performance: on ImageNet we match the reported accuracy, and on Places365, we observe only a 0.4% reduction.

Linear probe. We train a sparse linear classifier $h : \mathbb{R}^m \rightarrow \mathbb{R}^{|Y|}$ with ℓ_1 regularization:

$$\mathcal{L}_{\text{probe}} = \text{CE}(h(\hat{c}_i), y_i) + \lambda \|\omega\|_1, \quad (\text{B.16})$$

where ω are the probe weights, y_i is the class label of image i , CE is cross-entropy loss, and λ controls the L1 sparsity loss.

Training setup. We use AdamW optimizer [29] with $\beta_1 = 0.9$, $\beta_2 = 0.999$ and set the learning rate to $1e-4$. We use batch size of 1024 and train for 100 epochs, taking the highest accuracy checkpoint. For the hyper-parameter search, we perform the following sweep over a held-out subset (10% of training data).

$$\text{batch size} \in \{256, 512, 1024\}, \quad \text{learning rate} \in \{1e-3, 5e-4, 1e-4\}, \quad \lambda_{\text{L1}} \in \{0.1, 1.0, 2.0, 4.0, 8.0\}.$$

All other components (CLIP encoder ϕ , DINOiser g , SAE π and π^{-1}) remain frozen.

Thresholded variant. For the thresholded variant reported in the main paper, we set patch activations below a learned threshold to zero before pooling. The threshold per concept is set to match the BatchTopK sparsity: we use the k -th largest activation value observed during SAE training, where $k = 12$.

B.6. Image Captioning

To explore the capabilities of INSIGHT for downstream captioning task, we followed the setup of Mokady et al. [39], using the dense output tokens as prefix tokens to a language model. Specifically, we took the 14×14 dense tokens after SAE reconstruction, pooled them to 8×8 tokens, and fed them to a transformer adapter with learnable queries. The adapter has 8 layers with 10 learnable queries, which attend to the tokens from the vision encoder. The output for these 10 queries are then given to a pre-trained GPT-2 model [52] as prefix tokens.

Training. For Fig. 6 in the main paper, we trained the adapter and finetuned the language model on COCO captions [34], over train-, validation-, and test- subsets according to Karpathy splits. We found the suitable training checkpoint (epoch 5) and learning rate ($1e-4$) over the validation set and performed the final evaluation on the test set. We performed this both for INSIGHT as well as the baseline (same vision backbone without the SAE). We note that we kept the backbone vision model, as well as the concept representation (SAE) frozen (i.e., no fine-tuning) to this task.

C. Additional Results

In this section we extend the results provided in the main paper. We begin with concept visualizations for different concept families in Sec. C.1, as well as different matryoshka fractions in Sec. C.2. We then further demonstrate the downstream interpretability and utility of INSIGHT, with interpretable classification (Sec. C.3), interpretable open vocabulary segmentation (Sec. C.4), and steerable captioning (Sec. C.5).

C.1. Concept Families.

In Fig. C1, C2, C3, C5, C6, C4 we provide more curated examples from our family relation graph that show how families can deconstruct complex objects into their parts, that these families can have several levels of hierarchy and a concept can share multiple parents, that relationship can be based on concepts describing properties of another concept (e.g., material), and that relations can be abstract semantics (e.g., electricity, solar panel, and charging). With Fig. C5 we also show an example where relations are visually coherent, but naming can be limited, potentially because the concept vocabulary does not contain the relevant name or the text and image encoder of CLIP are not aligned for the specific fine-grained concept.

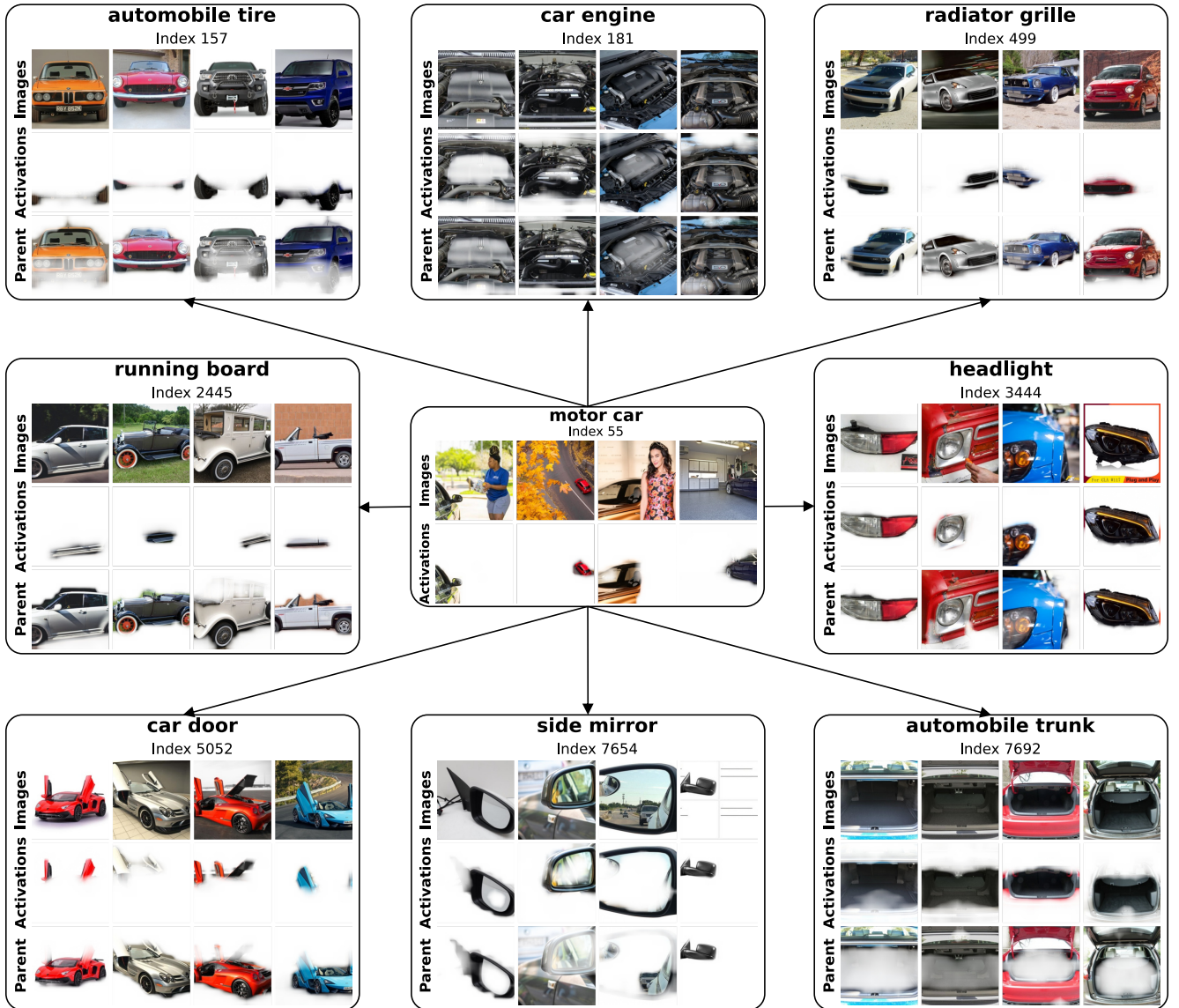


Figure C1. Families deconstruct complex objects into to their parts. Here we show a subgraph of the ‘motor car’ family to illustrate that family relationships can be formed as partonomies (part-based taxonomies). At the top of each concept visualization, we show the name and index of the concept, followed by a row of the top-activating images and their corresponding concept activation regions. For concepts with parents, we also show the parent activation on the same image below.

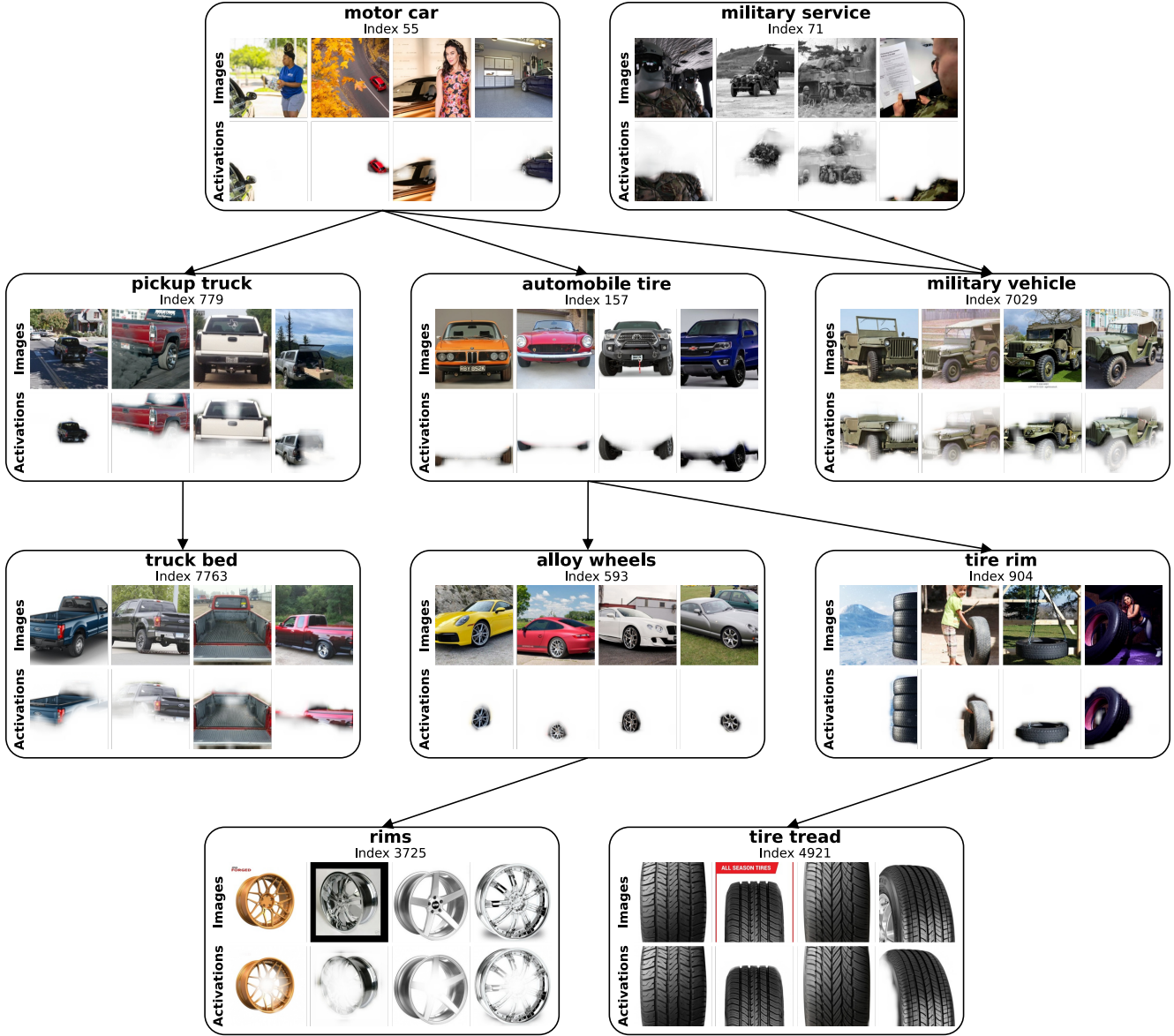


Figure C2. **Concept families have a DAG structure.** We show a subgraph of the "motor car" family that shows the complexity of discovered families with several levels in the hierarchy and concepts having multiple parents (see 'military vehicle' with two parents 'motor car and 'military service'). Furthermore, the family also reveals progressively finer-grained concepts, such as 'alloy wheels' (third row) and the even finer subpart 'rim' (fourth row).



Figure C3. **Families can be semantically highly coherent.** We show the entire "vineyard" family, i.e. the concept "vineyard" with all of its descendants and ancestors in the Family graph \mathcal{G} . A family of acquired taste.

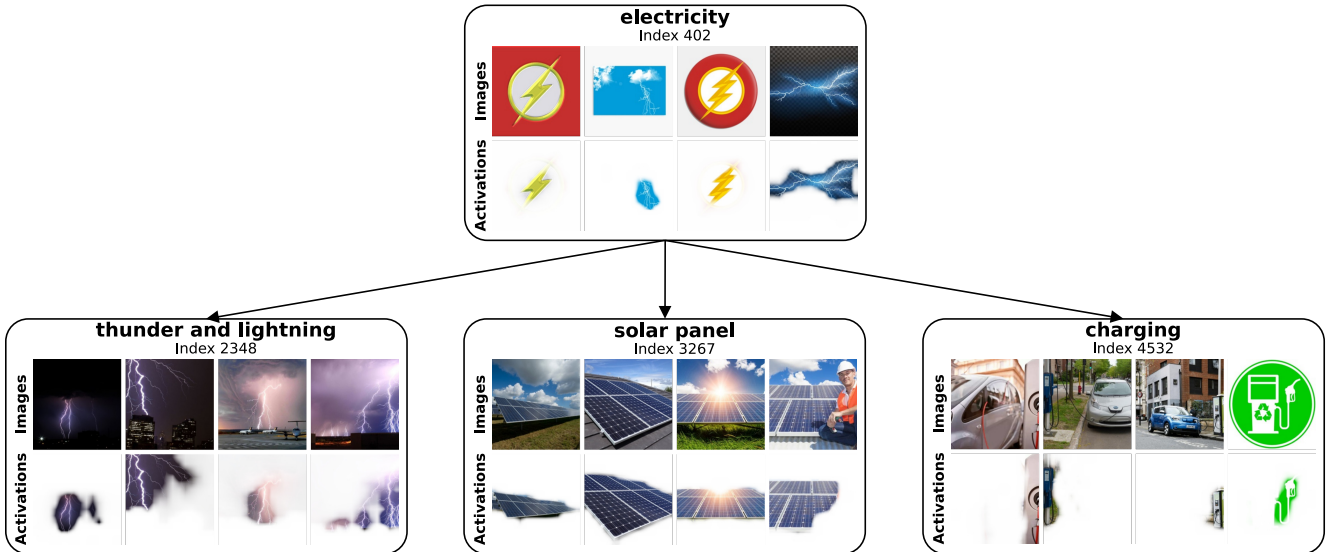


Figure C4. **Families can have abstract semantic relationships, without any common visual patterns.** We show the full "electricity" family. Note that children like "solar panel" or "charging" do not share visual patterns with the top-activating examples of the parent "electricity", but instead are connected through an abstract semantic relationship.

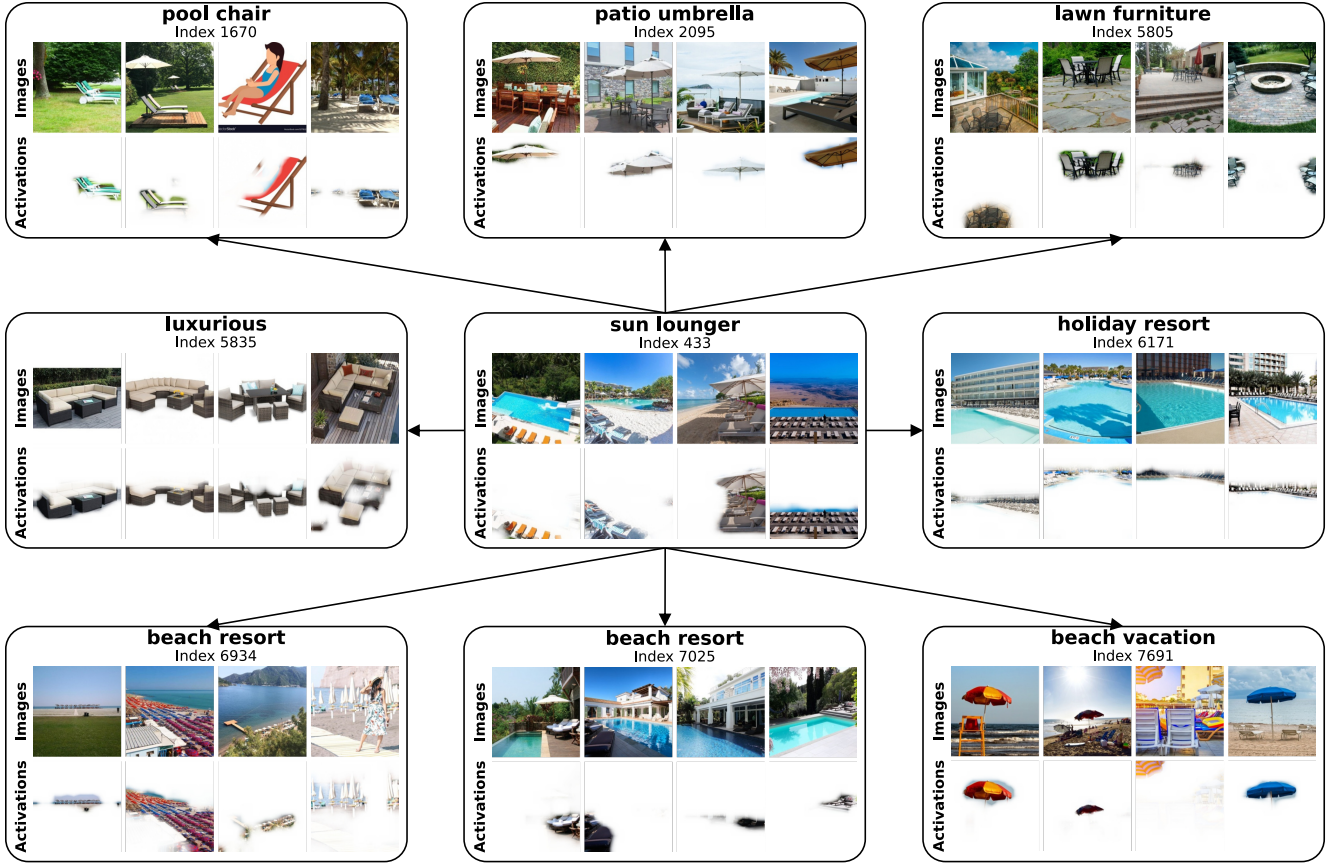


Figure C5. **Concept naming can be limited in the context of families.** We show the entire "sun lounger" family with all of its descendants in the Family graph \mathcal{G} . We observe that while the concept relations do make sense and concepts are spatially well grounded, concept naming is not ideal with multiple descendants receiving overly general names.



Figure C6. **Families can be based on material properties.** We show the entire "vintage lace" family from the Family graph \mathcal{G} . We find both specifications as well as sub-material relationships ("is made of").

C.2. Random Concept Visualization.

We further show a random selection of concepts for each Matryoshka group in Fig. C7 and observe that concepts are easy to understand, spatially well located, and correspond to frequent to less frequently used concepts.

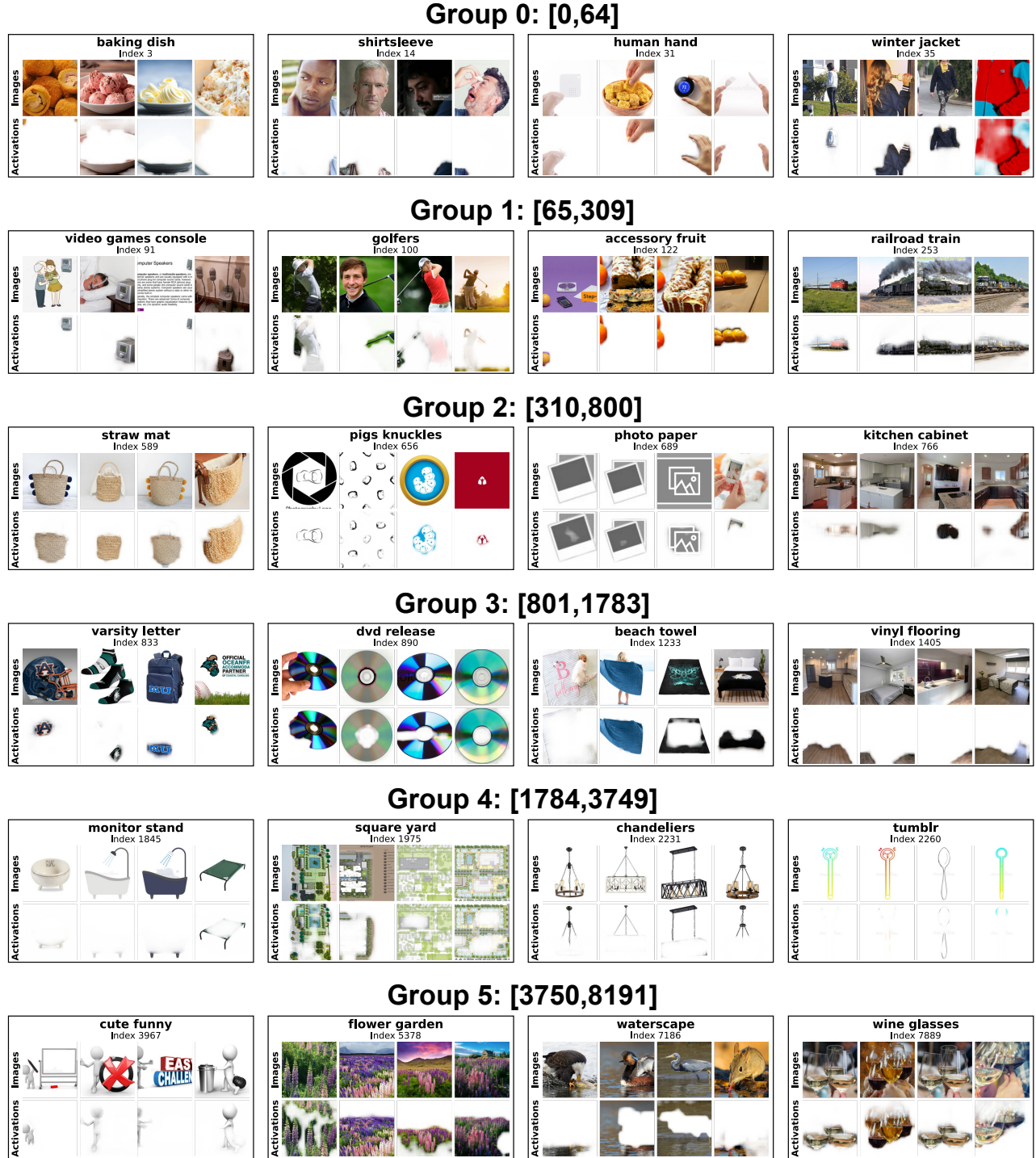


Figure C7. **Randomly sampled Concepts per Matryoshka group.** We show a random selection of concepts in each Matryoshka shell, defined by a range of neuron indices. By design of the Matryoshka training, the lower the range, the more "general" the information.

C.3. Interpretable Classification

Here, we provide additional qualitative results explanations for classifications on ImageNet (Fig. C8) and Places365 (Fig. C9) and observe that explanations are rooted in spatially well-grounded fine-grained relevant concepts. Moreover, in contrast to many existing works, the top concepts cover a large fraction of the overall relevance for a classification, meaning the explanations are succinct, which is a natural consequence of using (batch) top-k SAE architectures.

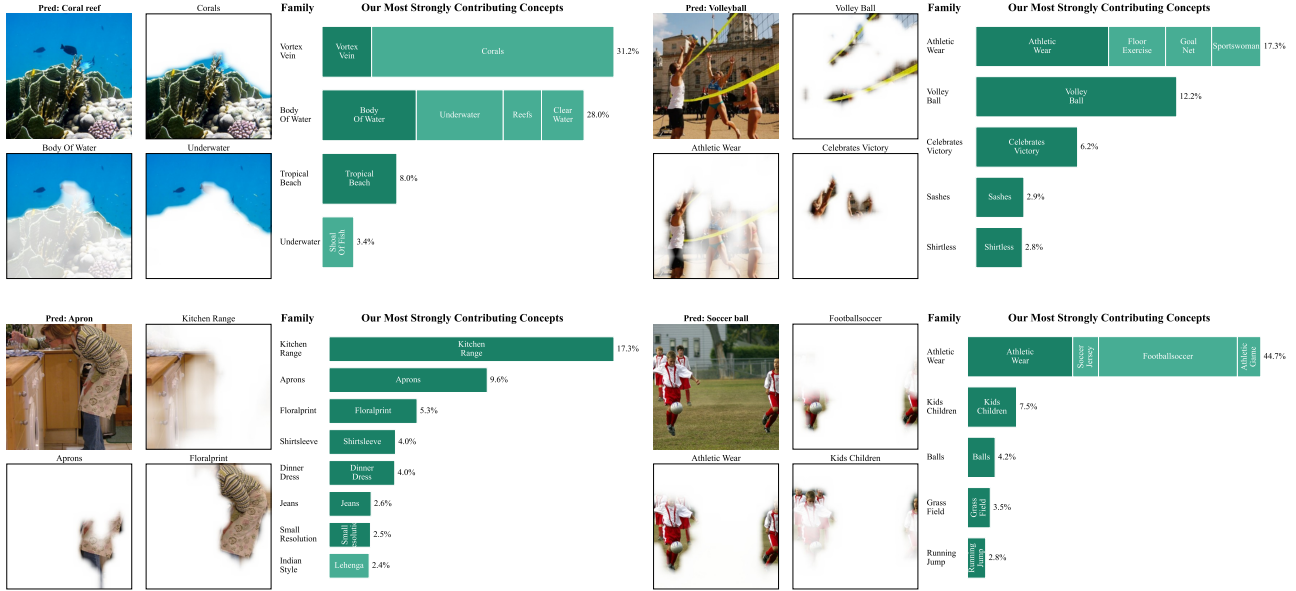


Figure C8. **Spatial grounding of concept-based explanations for Imagenet.** We provide example images, their predicted class, along with fine-grained concept-based explanations showing contributions to prediction as bar plots, and spatial grounding in terms of per-patch concept activations.

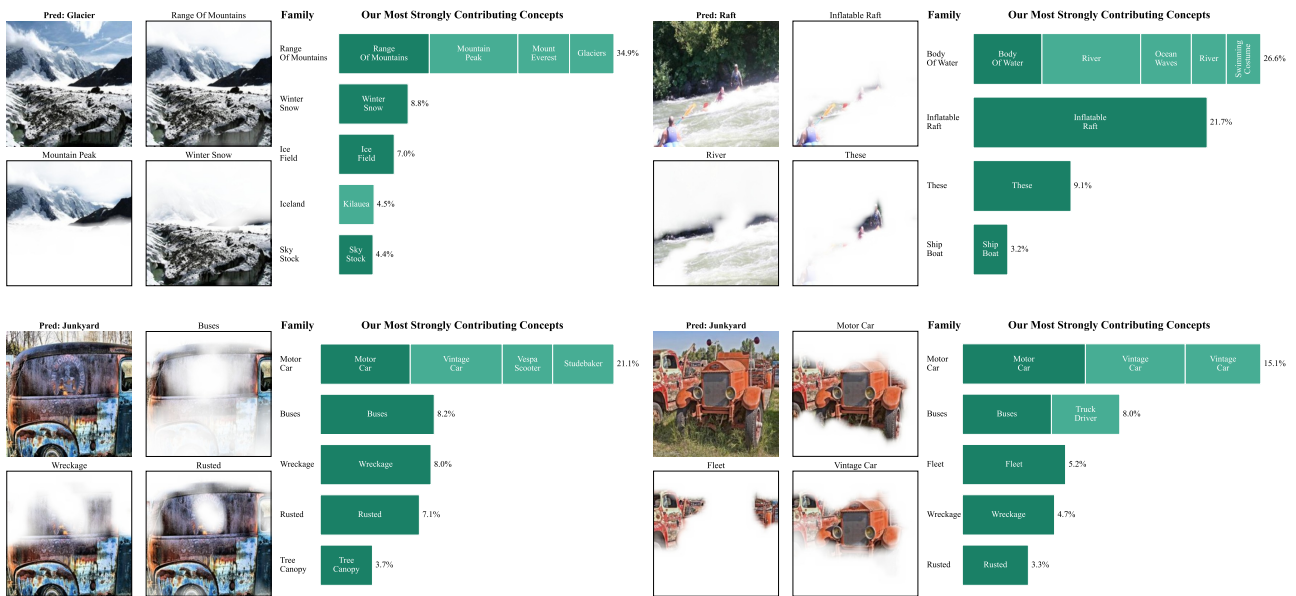


Figure C9. **Spatial grounding of concept-based explanations for Places365.** We provide example images, their predicted class, along with fine-grained concept-based explanations showing contributions to prediction as bar plots, and spatial grounding in terms of per-patch concept activations.

C.4. Interpretable Open Vocabulary Segmentation

Here in Figs. C10 and C11, we provide additional qualitative explanations for Open Vocabulary Segmentations (OVS) on PASCAL-VOC [20], Coco-Object [7], COCO-Stuff [7], and ADE20K [75]. Note that in contrast to existing work, we can decompose the patch-wise segmentation logits into concept-wise contributions to the text label.

ADE20k

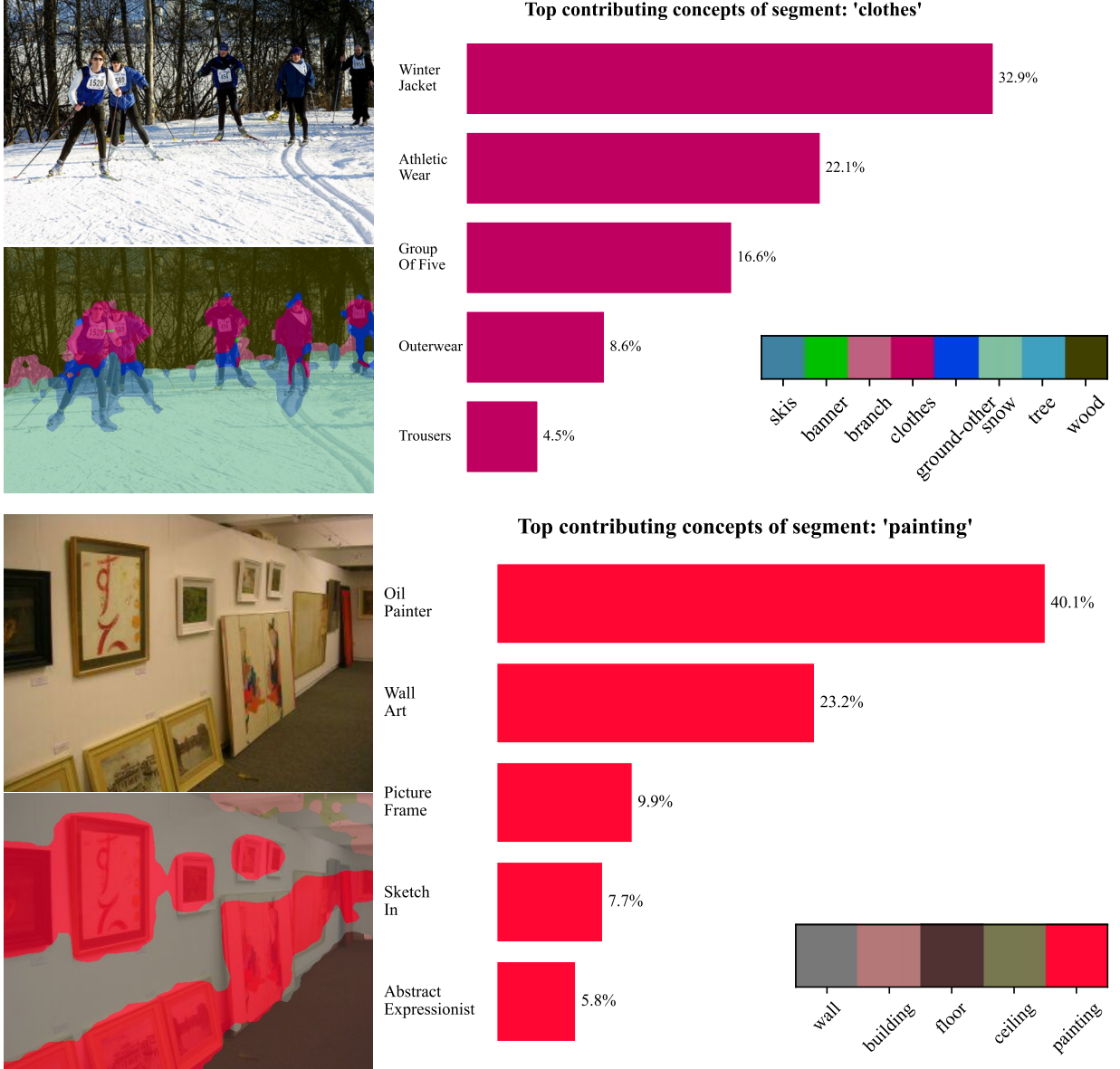
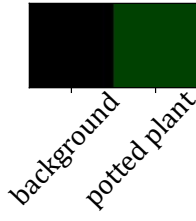
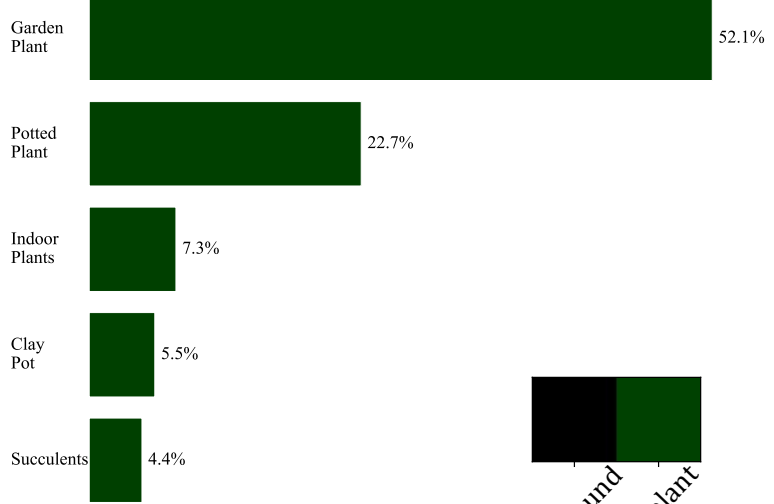


Figure C10. **INSIGHT enables interpretable open-vocabulary segmentation.** Top left: input image. Bottom left: segmentation produced by INSIGHT when provided with the full set of dataset label names as text queries. Top right: bar plot showing the top contributing concepts for a selected segmentation label, where contribution is computed as the product of concept activation and its cosine similarity with the label embedding. Bottom right: all segmentation labels that the model identifies as present in the image. This illustrates how INSIGHT produces both pixel-level predictions and transparent concept-level explanations of why each label is selected.

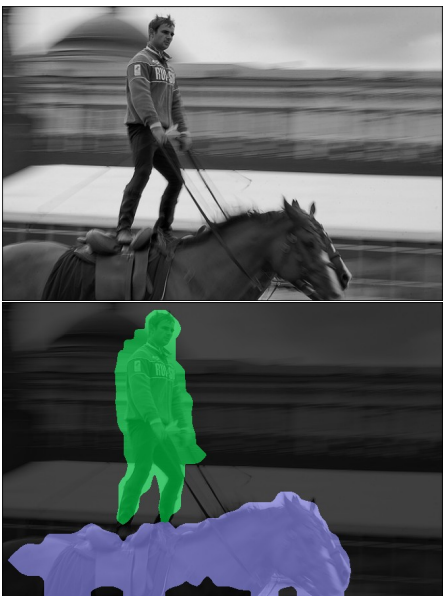
VOC



Top contributing concepts of segment: 'potted plant'



COCO-Object



Top contributing concepts of segment: 'person'

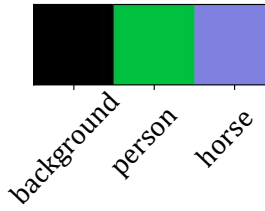
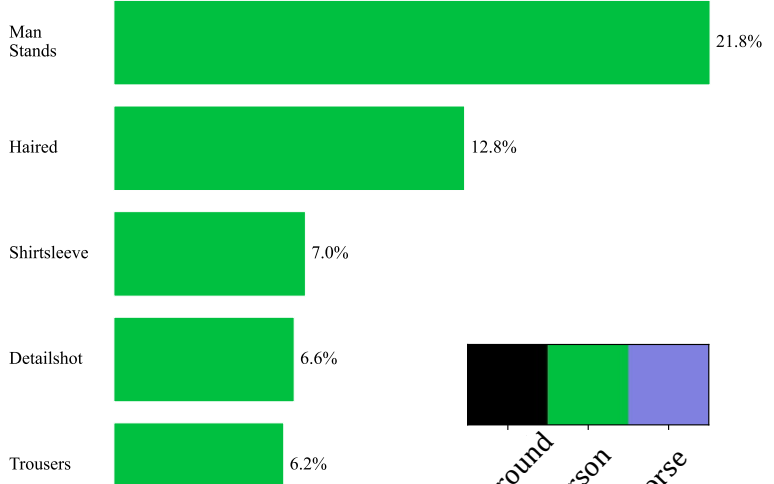


Figure C11. **INSIGHT enables interpretable open-vocabulary segmentation with background removal.** We demonstrate segmentation results when providing INSIGHT with the full set of dataset label names together with an additional background prompt. The background label is used to filter out non-foreground regions, allowing the model to focus on semantically meaningful segments. As in the main results, INSIGHT produces both pixel-level segmentations and concept-level explanations through contribution scores derived from concept activations and their cosine similarity with the corresponding label embeddings.

C.5. Steerable Captioning

Here we extend the qualitative results for captioning and steering shown in the main paper with additional samples. In Fig. C12 we show unseen test samples from the COCO dataset [34], and report the model captions before and after steering. The concepts were selected by a direct look up of the underlined terms, over the automatically assigned names.

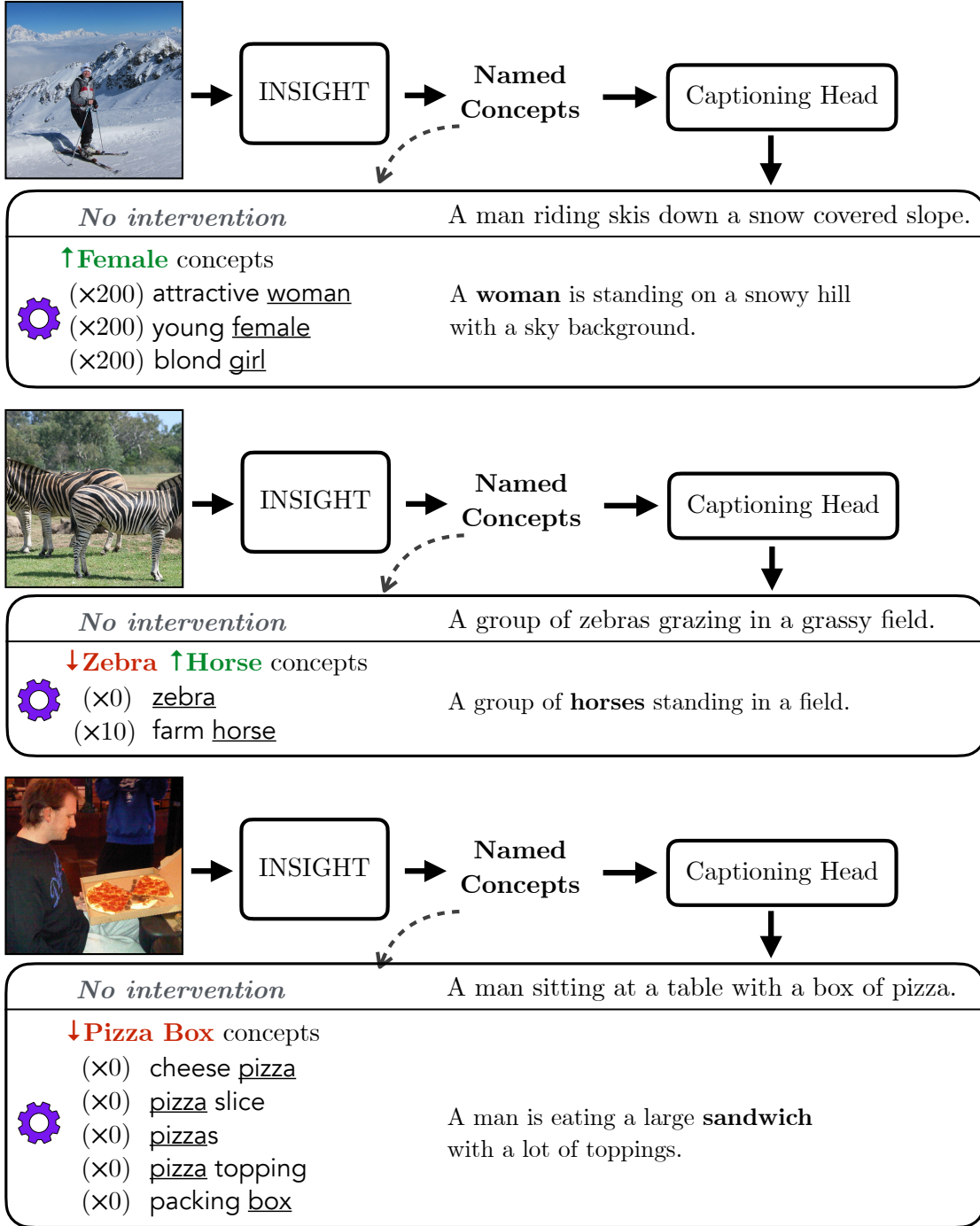


Figure C12. **A simple proof of concept for steering with INSIGHT.** In each example (major rows), we steer the output caption through intervention on the concept activations (left), e.g. ‘zebra’ activations are multiplied by zero in the middle row. The concepts were selected by a simple look up over automatically assigned names for the activated concepts (matched term is underlined for each concept). We observe that the intervention is effective in steering the output caption, highlighting the utility of a concept-based bottleneck representation and the high quality of the concept naming.